3-4-2005

Electrical Activation Studies of Silicon Implanted $Al_xGa_{1-x}N$

Timothy W. Zens

ELECTRICAL ACTIVATION STUDIES OF SILICON IMPLANTED
$Al_xGa_{1-x}N$

THESIS

Timothy W. Zens, 2nd Lieutenant , USAF

AFIT/GAP/ENP/05-08

DEPARTMENT OF THE AIR FORCE
AIR UNIVERSITY

AIR FORCE INSTITUTE OF TECHNOLOGY

Wright-Patterson Air Force Base, Ohio

APPROVED FOR PUBLIC RELEASE; DISTRIBUTION UNLIMITED

The views expressed in this thesis are those of the author and do not reflect the official policy or position of the United States Air Force, Department of Defense, or the United States Government.

ELECTRICAL ACTIVATION STUDIES OF SILICON IMPLANTED $Al_xGa_{1-x}N$

THESIS

Presented to the Faculty

Department of Engineering Physics

Graduate School of Engineering and Management

Air Force Institute of Technology

Air University

Air Education and Training Command

in Partial Fulfillment of the Requirements for the

Degree of Master of Science (Applied Physics)

Timothy W. Zens, BS

2nd Lieutenant , USAF

March 2005

APPROVED FOR PUBLIC RELEASE; DISTRIBUTION UNLIMITED

ELECTRICAL ACTIVATION STUDIES OF SILICON IMPLANTED $Al_xGa_{1-x}N$

Timothy W. Zens, BS
2nd Lieutenant , USAF

Approved:

Yung K. Yeo (Chairman)   4 March 05
                                       date

Robert L. Hengehold (Member)   4 Mar '05
                                       date

James A. Fellows (Member)   4 MAR 05
                                       date

Abstract

Electrical activation studies of silicon implanted $Al_xGa_{1-x}N$ grown on sapphire substrates were conducted as a function of ion dose, anneal temperature, and anneal time. Silicon ion doses of $1x10^{13}$, $5x10^{13}$, and $1x10^{14}$ cm^{-2} were implanted in $Al_xGa_{1-x}N$ samples with aluminum mole fractions of 0.1 and 0.2 at an energy of 200 keV at room temperature. The samples were proximity cap annealed at temperatures from 1100 to 1350 ℃ and anneal times of 20 to 40 minutes with a 500 Å thick AlN cap in a nitrogen environment. The Hall coefficient and resistivity were measured using room temperature Hall effect measurements. From this data the Hall mobility, sheet carrier concentration, and electrical activation efficiencies were calculated.

Activation efficiencies of almost 100% were achieved for $Al_{0.2}Ga_{0.8}N$ samples having doses of $5x10^{13}$ and $1x10^{14}$ cm^{-2} after annealing at 1350 and 1300 ℃, respectively, for 20 minutes. After annealing at 1250 ℃ for 20 minutes, 87% efficiency was achieved for $Al_{0.1}Ga_{0.9}N$ implanted with $1x10^{14}$ cm^{-2} silicon ions. The largest observed mobility was 89 $cm^2/V{\cdot}s$ for $Al_{0.1}Ga_{0.9}N$ implanted with $1x10^{14}$ cm^{-2} and $5x10^{13}$ cm^{-2} silicon ions and annealed at 1250 ℃ for 20 minutes and at 1200 ℃ for 40 minutes, respectively.

The optimal anneal condition to maximize electrical activation efficiency and minimize nitrogen dissociation damage for $Al_{0.1}Ga_{0.9}N$ was 1200 ℃ anneal for 40 minutes. The mobilities, sheet carrier concentrations, and electrical activation efficiencies generally increased.

iv

Acknowledgments

Table of Contents

List of Figures

viii

List of Tables

ELECTRICAL ACTIVATION STUDIES OF SILICON IMPLANTED AlxGa1-xN

I. Introduction

1.1 Overview

Electrical properties of silicon implanted $Al_xGa_{1-x}N$ grown on sapphire substrates were studied as a function of ion dose, anneal temperature, and anneal time. $Al_xGa_{1-x}N$ samples with aluminum mole fractions of 0.1 and 0.2 were implanted with silicon ions at 200 keV at room temperature. The samples were proximity cap annealed with a 500 Å thick AlN cap in a nitrogen environment. Anneal temperatures ranged from 1100 to 1350 ℃ and anneal times varied from 20 to 40 minutes. Room temperature Hall effect measurements were used to determine the Hall coefficient and resistivity. From this data the Hall mobility, sheet carrier concentration, and electrical activation efficiencies were calculated. The primary objective is to discover anneal conditions that produce activation efficiencies on the order of 80-100% and occur at commercially viable temperatures. The secondary goal of this research is to discover the optimal anneal time and temperature for recovery of damage caused by ion implantation.

There has been extensive research into recovering damage in GaN due to ion implantation. Specifically, activation efficiencies of 90 and nearly 100% have been reached for silicon ion doses of $5x10^{15}$ cm^{-2} implanted at 100 and 200 keV ions and annealed at 1400 ℃ for 10 seconds and 1350 ℃ for 2 minutes respectively

1

[1:229;2:1930]. Less work has been done on $Al_xGa_{1-x}N$'s optimal annealing conditions. For 200 keV silicon ion doses of $5x10^{14}$ cm^{-2} in $Al_{0.18}Ga_{0.82}N$ an activation efficiency of nearly 100% and 94% was observed for a dose of $1x10^{15}$ cm^{-2} after annealing at 1250 ºC and 1200 ºC for 25 min respectively[3:6277]. However, for lower doses on the order of $1x10^{14}$ to $1x10^{13}$ cm^{-2} the results have been less successful. Previously, activation efficiencies of 40, 65, and 70% have been observed in GaN implanted with and $1x10^{13}$, $5x10^{13}$, and $1x10^{14}$ cm^{-2} annealed at 1350 ºC for 17 seconds[17:118]. For $Al_{0.2}Ga_{0.8}N$ an activation efficiency of 60% was achieved with a silicon ion dose of $1x10^{14}$ cm^{-2} annealed at 1350 ºC for 2 minutes [8:46]. However, there has not been a complete exploration of the optimum annealing conditions of low dose $Al_{0.1}Ga_{0.9}N$.

Hall Mobilites of 65 $cm^2/V\cdot s$ have been obtained in $Al_{0.18}Ga_{0.82}N$ implanted with $1x10^{15}$ cm^{-2} 200keV silicon ions annealed at 1250 ºC for 25 minutes[3:6279]. However, for lower doses lower Hall mobilies of nearly 30 $cm^2/V\cdot s$ have been observed in $Al_{0.18}Ga_{0.82}N$ implanted with $1x10^{14}$ cm^{-2} 200keV silicon ions annealed at 1350 ºC for 2 minutes[8:44]. Moreover, there has not been a thorough exploration of the Hall Mobilities of low dose $Al_{0.1}Ga_{0.9}N$.

The current semiconductor market is dominated by the silicon because it is cheap to grow in bulk and it works well at room temperature. Because silicon has been so important to the emerging semiconductor industry, its properties have been richly researched and developed. All of this research has shown where silicon is limited. Due to its smaller band gap energy, silicon can not function under high temperatures, high electric fields, and high frequency electronic ranges. Also, silicon's indirect band gap gives it a low absorption coefficient and makes it a poor light emitter.

2

Where silicon is weak, group III-nitrides are strong. Group-III nitrides have high thermal conductivities which allow them to dissipate heat. Alloys of group III-nitrides such as $Al_xGa_{1-x}N$ possess a very wide band gap which makes them ideal for extreme power, temperature, and frequency applications. In addition, the alloy $Al_xGa_{1-x}N$ has high cohesion energy which gives this semiconductor the ability to function in caustic environments and reduces its vulnerability to radiation damage.

These strengths of group III-nitrides also have DoD applications. The ability of these semiconductors to function at high power makes them ideal for use in high-power amplifiers, diodes, and switches. Their high temperature applications allow these semiconductors to be used in munitions and aircraft engines. Since group III-nitrides are naturally resistant to radiation damage and can function in large electric fields, they are well suited for use in satellites. Other DoD applications include threat warning systems, lasers, imaging, solar blind photo diodes, and more[4:285;5:1363].

1.2 Challenges

Despite all of the capabilities that group III-nitrides possess, there is little consensus on the proper ion implantation doping and annealing techniques. The two major methods of doping $Al_xGa_{1-x}N$ are in-situ doping and ion implantation. In-situ doping takes place at high temperatures that inhibit good crystal growth [6:55]. It is also very time consuming and therefore expensive. On the other hand, the process of ion implantation significantly damages the crystal structure. Therefore it is necessary to anneal out this damage.

3

Work done in the past has shown that annealing at 1350 ℃ removes ion implantation damage [7:x] and allows up to 90% electrical activation efficiency [8:ix]. However, temperatures of this magnitude are highly impractical for commercial fabrication. Moreover, recent research [9:1] shows that $Al_{0.18}Ga_{0.82}N$ has almost 100% electrical activation efficiency when annealed at 1250 ℃ for 25 minutes with a silicon dose of $5x10^{14}$ cm^{-2}. Previous work has shown that at these temperatures, damage due to implantation is not fully removed [7:x]; however the evidence shows that electrical activation efficiency remains high [8:46].

4

2.1 $Al_xGa_{1-x}N$ Properties and Applications

$Al_xGa_{1-x}N$ and other wide band gap semiconductors have been used to produce blue-UV laser diodes, UV detectors, and light emitting diodes. New $Al_xGa_{1-x}N$ applications will arise because of the material's unique properties. Chief among these are $Al_xGa_{1-x}N$'s large break down voltages, high saturation velocities, high thermal conductivities, and large cohesion energies. $Al_xGa_{1-x}N$ can be used in high power amplifier, switches, and diodes because of its large breakdown voltage. This property is due to $Al_xGa_{1-x}N$'s wide band gap; the breakdown voltage of a semiconductor is proportional to its band gap to the three halves power [8:3]. A wide band gap is also the reason for $Al_xGa_{1-x}N$'s high saturation velocity. A higher saturation velocity makes $Al_xGa_{1-x}N$ ideal for high frequency applications like high electron mobility field effect transistors [10:2; 11:2535]. $Al_xGa_{1-x}N$ has a high thermal conductivity when compared to other semiconductors which allows it to quickly dissipate junction heat. This property is particularly useful for high temperature applications like high power lasers which could operate at wavelengths of just above 200 nm. The large cohesion energy of group III-nitrides like $Al_xGa_{1-x}N$ makes them ideal for operation in caustic or radioactive environments. Finally, group III-nitrides are desirable for use in optoelectronic devices because they have direct band gaps.

A specific comparison of GaN to the properties of several other semiconductors is shown [17:2] in Table 1.

5

Table 1. Comparisons of semiconductor materials and properties

Property	Si	GaAs	InP	4H-SiC	GaN	Diamond
Bandgap at 300 K (eV)	1.12 (I)	1.424 (D)	1.344 (D)	3.26 (I)	3.44 (D)	5.47 (I)
Dielectric constant	11.7 (dc)	13.2 (dc) 10.9 (∞)	12.4 (dc) 9.66 (∞)	9.6 (dc) 6.7 (∞)	8.9 (dc) 5.35 (∞)	5.57 (dc)
Thermal expansion ($\times 10^{-6}$ K$\cdot\Delta$a/a)	2.56	6.86	4.5	4.2	5.59	0.08
Lattice constant (Å)	5.431	5.653	5.869	3.073 (a) 10.05 (c)	3.189 (a) 5.185 (c)	3.567
m_c^*/m_o	1.18	0.063	0.077	-	0.22	0.2
m_v^*/m_o	0.81	0.53	0.64	-	0.8	0.25
Bulk Mobility Electron Hole	1450 500	8500 400	4600 150	1140 50	900 150	2200 1600
Saturation velocity ($\times 10^7$ cm/sec)	1.0	1.0	-	2.0	2.5	2.7
Breakdown field (MV/cm)	0.3	0.4	-	3	5	10
Thermal conductivity (W/cm·K)	1.5	0.46	0.68	4.9	1.3	22
Melting Point (°C)	1412	1238	1070	Sublimes T > 1827	Sublimes T > 1300	3826

2.2 Crystal Structure

In a solid there are only three different types of matter organization [6:9] amorphous, single crystalline, and polycrystalline. In an amorphous organization the solid is arranged randomly. A single crystalline organization has a periodic organization that is well defined all the way through the crystal. A polycrystalline arrangement corresponds to an ordered arrangement of atoms in sections which differ in their orientation through the crystal. The three different crystalline organizations are shown [6:10] in Figure 1.
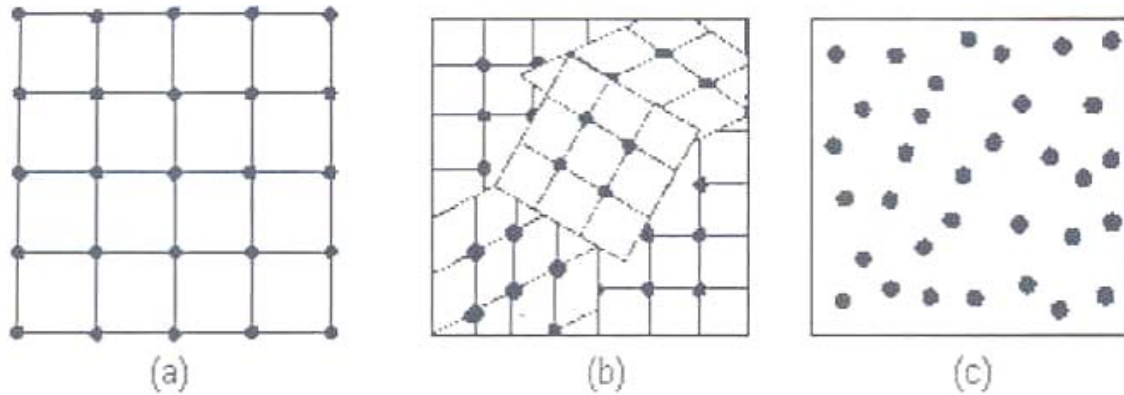
Figure 1. The three types of crystal organizations: single crystalline (a), polycrystalline (b), and amorphous (c).

Semiconductors have single crystalline arrangements and of the 14 possible single crystalline arrangements nearly all are arranged in the cubic or hexagonal symmetry groups. Each lattice has a unit cell which is reproduced throughout the crystal [12:7]. The length of that unit cell is called the lattice constant and is unique for each group III-nitride.

All epitaxially grown group III-nitrides crystallize in zincblende and wurtzite structures. Both structures are tetrahedrally bonded, however, the zincblende structure is made up of two interpenetrating face centered cubic Bravais lattices and the wurtzite structure consists of two interpenetrating hexagonal Bravais lattices. The structure of these two crystal formations is shown [13:9] in Figure 2.

7
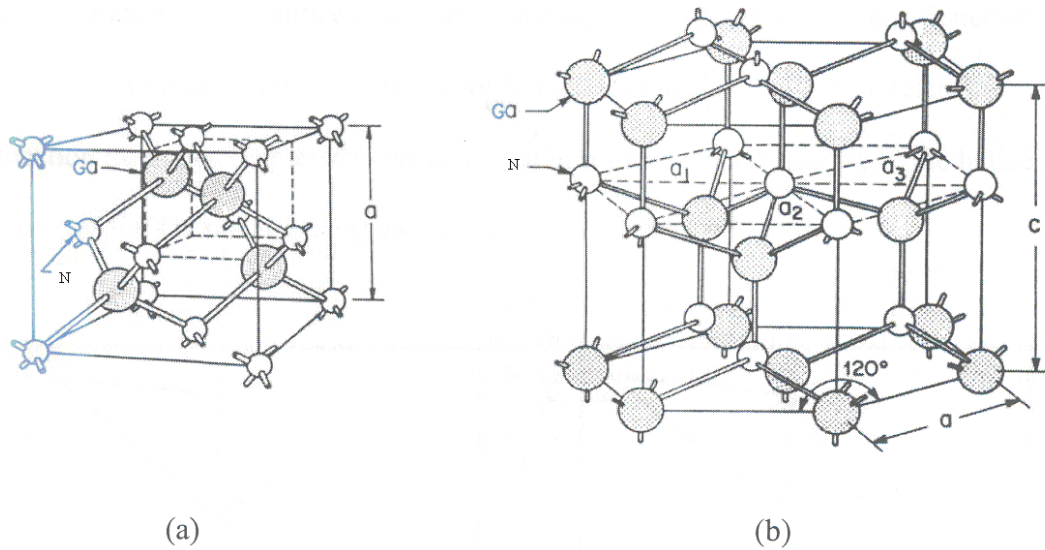
Figure 2. The two common types of semiconductor crystal organizations:
zincblende (a) and wurtzite (b).

There are three different types of intrinsic point defects that can exist in a crystal: interstitials, vacancies, and antisites. An interstitial is when an atom, which was not supposed to be in the crystal structure at all, comes to rest between lattice positions. A vacancy arises when a position in a crystal is left unfilled. An antisite is formed when one of the atoms that is supposed to be in the crystal is in the wrong position. For example if nitrogen is in a lattice position that is meant to be occupied by gallium in GaN then nitrogen is an antisite defect.

Other imperfections arise when producing an alloy of two group III-nitrides. If one type of semiconductor is to be grown on top of another, the lattice constants must be very close. The lattice constant defines the size of the unit cell. The zincblende structure, which is cubically symmetric, is described by one lattice constant represented in Figure 2 as "a". The wurtzite structure on the other hand, is hexagonally symmetric

8

and is described by two lattice constants represented as "a" and "c".   As can be seen [6:25] in Figure 3, severe atomic misfit will result in unpaired atoms in the lattice. On the other hand, a minor misfit will only strain the bonds but each atom will be paired.
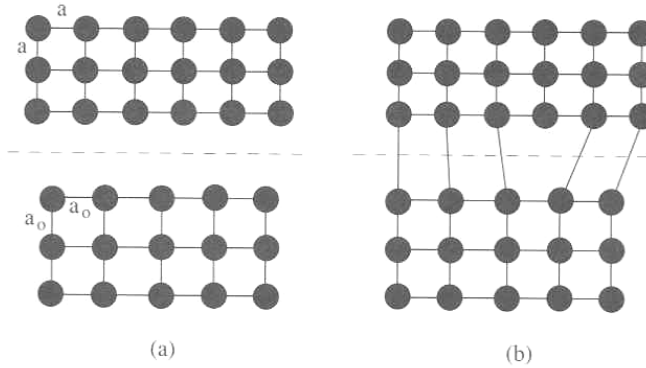
Figure 3. The defects caused by a lattice mismatch seen before (a) and after (b) bonds are formed.

The complex defects caused by lattice mismatch are known as dislocation lines. The lattice constants of AlN and GaN are within 2.4% of each other, as can be seen [6:33] in Figure 4.
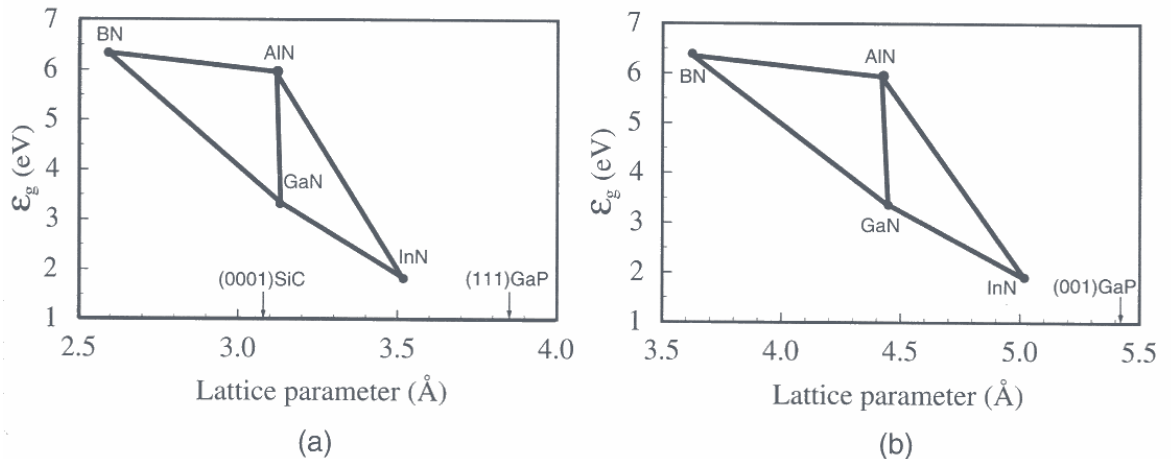
Figure 4. The lattice constants and band gaps of nitride structures in (a) wurtzite and (b) zincblende crystal structure.

9

2.3 Semiconductor Basics

Normally, if an atom is separated from other atoms, its electronic energy levels are discrete. However, as can be seen [14:2] in Figure 5, when the atomic separation decreases the degenerate energy levels become continuous bands. The lower energy band is called the valance band and the higher energy band is known as the conduction band. When the material is at absolute zero, all electrons are in the valence band. However, as the temperature increases some electrons may be thermally excited into the conduction band.
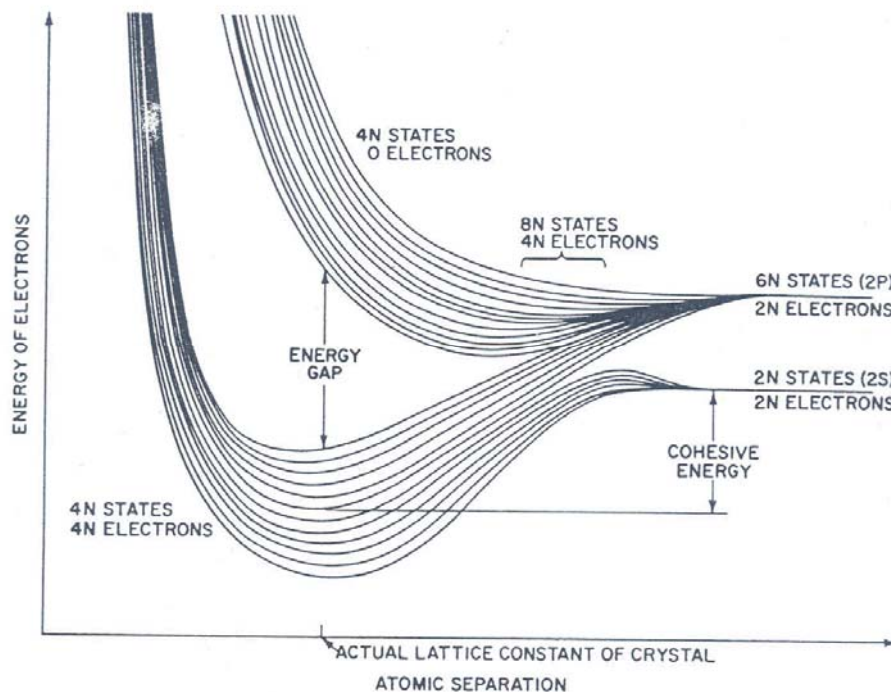
Figure 5. Behavior of energy levels with decreasing inter-atomic distances.

The energy separation of the valence and conduction bands determines the conductivity of the material. Materials whose valance and conduction bands are overlapping are called conductors because it is very easy to move electrons through the

material. An insulator has an extremely large band gap and it is nearly impossible to send current through the material. Finally, semiconductors are materials whose valence and conduction bands are not over lapping, however, the band gap energy is small enough so electrons can be thermally excited into the conduction band. The band gap energy of semiconductors ranges from a few meV to a little less than 6.3 eV. For $Al_xGa_{1-x}N$ it ranges from 3.4-6.2 eV depending on aluminum mole fraction.

A semiconductor that is made up of one type of atom, such as silicon, is an elemental semiconductor. The semiconductors being studied in this research are compound semiconductors, specifically group III-nitrides. Group III-nitrides get their name because one of the constituents is in the third column of the periodic table, which means these elements have three valance electrons. $Al_xGa_{1-x}N$ is an alloy of two group III-nitrides, where x represents the aluminum mole fraction.

The band gap for $Al_xGa_{1-x}N$ at room temperature is given as:

$$E_g(x) = xE_g(AlN) + (1-x)E_g(GaN) - bx(1-x), \qquad (1)$$

where $E_g(GaN)$=3.39 eV at room temperature, $E_g(AlN)$=6.20 eV at room temperature, and b=1.0±0.3 eV at room temperature. Here, b is the bowing parameter [6:20].

A semiconductor which contains no impurities is known as an intrinsic semiconductor. At a given temperature some electrons will be thermally excited into the conduction band. The concentration of these excited electrons is known as the intrinsic carrier concentration.   Since the group-III nitrides have various band gap energies, their intrinsic carrier concentrations also vary. Each thermally excited electron leaves a

11

vacancy when it is excited into the conduction band. These vacancies are known as holes and are treated as positive charge carriers.
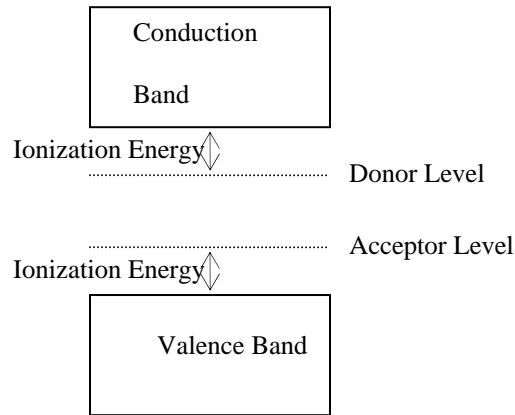
Figure 6. Energy band diagram for a semiconductor.

When impurity atoms are added to a semiconductor, the semiconductor is called extrinsic. The impurities inserted into the semiconductor can either be acceptors or donors. The energy levels of these impurities are shown in Figure 6. At absolute zero the electrons from donor impurities and holes from acceptor impurities are tightly bound to their respective impurity atoms. It takes less energy to thermally excite electrons into the conduction band from the donor impurity than it does to excite electrons lying in the valence band. Likewise, electrons in the conduction band give up less energy by recombing with holes in the acceptor impurity as opposed to holes in the valance band.

When temperature is lower, below 70 K for $Al_{0.2}Ga_{0.8}N$ [8:47], the only electrons in the conduction band come from the donor level. This is called extrinsic conductivity. On the other hand when temperature gets higher, valence band to conduction band transitions become dominant. This conductivity is intrinsic.

12

2.4 Band Structure

When the spacing between the atoms in a solid becomes less than about 2 Å the wave functions of the outer electrons in the valance band overlap and form an electron cloud. The innermost electrons remain close to the nucleus and shield the cloud of valance electrons from the attractive force of the nucleus. As is illustrated in Figure 5, the discrete degenerate energy levels of valance electrons form a continuous band. The energy of the valance and conduction bands vary as the wave vector $\vec{k}$ changes. The band diagrams of GaN and AlN are shown [15:8135; 16:413] in Figure 7.
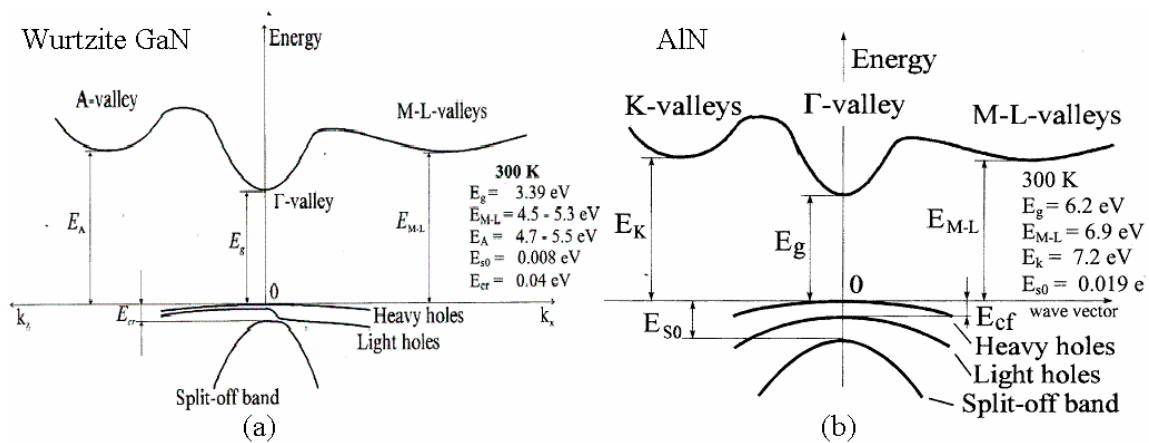
Figure 7. The band structure of (a) wurtzite GaN and (b) AlN.

If the conduction band reaches its minimum and the valance band reachs its maximum value when $\vec{k} = 0$, then the semiconductor has a direct band gap. This point is referred to as Γ=0. When this does not occur the semiconductor is said to have an indirect band gap. As can be seen in Figure 7, the valance and conduction bands can be approximated as parabolas.

13

The equations of the parabola for the conduction band near $\Gamma=0$ is given as:

$$E(k) = E_g + \frac{\hbar^2 |\vec{k}|^2}{2 \cdot m_e {}^*} \tag{2}$$

and for the valance band near $\Gamma=0$ the equation becomes:

$$E(k) = \frac{-\hbar^2 |\vec{k}|^2}{2 \cdot m_h {}^*}, \tag{3}$$

where $E(k)$ represents the energy of the conduction band and valance band, respectively. E_g corresponds to the band gap, $\hbar$ is planck's constant; $m_e{}^*$ and $m_h{}^*$ are the effective masses of electrons in the conduction band and holes in the valance band, respectively. The values for the effective mass are found by using the following relations

$$m_e {}^* = \frac{\hbar^2}{d^2 E_c / d|\vec{k}|^2} \tag{4}$$

and

$$m_h {}^* = \frac{\hbar^2}{d^2 E_v / d|\vec{k}|^2}. \tag{5}$$

In order to find out how many electrons are within a certain energy range, the product of the Fermi-Dirac and the density of states function must be integrated over the desired energy range. The probability of finding an electron at a given energy is described by the Fermi-Dirac distribution, which is:

$$f(E) = \frac{1}{\exp\left[\dfrac{E - E_F}{k_B T}\right] + 1}, \tag{6}$$

where E_F is the energy at which the probability of an electron occupying this state is 50%, T is the temperature, and k_B is Boltzman's constant. The energy E is measured from the

14

bottom of the conduction band. The distribution function of the valance and conduction

bands is given by:

$$g_{c,v}(E) = \frac{\sqrt{2|(E - E_{c,v})|}}{\pi^2 \hbar^3}(m_{e,h}*)^{3/2},$$ (7)

where E_c and E_v are the energies of the valance and conduction bands at $\Gamma=0$,

respectively. Finally, one of the properties of semiconductors that was investigated in

this research is the mobility of $Al_xGa_{1-x}N$. Mobility, μ, is the average drift velocity per

unit field; it is a measure of how easily charge carriers can move through a solid. If the

mobility of a semiconductor is known, the conductivity, σ_e, is given by:

$$\sigma_e = n \cdot q \cdot \mu_e.$$ (8)

2.5 Molecular Beam Epitaxy (MBE)

MBE is the process used to grow all of the semiconductors used in this research.

The setup of a typical MBE system is shown [8:16] in Figure 8. A substrate, on which

the crystal will be grown, is placed on the rotating substrate holder. In this research, the

lattice constant of the $Al_xGa_{1-x}N$ crystal and the Al_2O_3 substrate are significantly

different. This difference -- often more than 10% -- places tensile and biaxial strain on

the crystal. Because strain is directly proportional to the degree of the lattice mismatch, a

buffer layer is often placed on the substrate to reduce the degree of mismatch. This

research used a sapphire substrate and a thin AlN buffer.

15
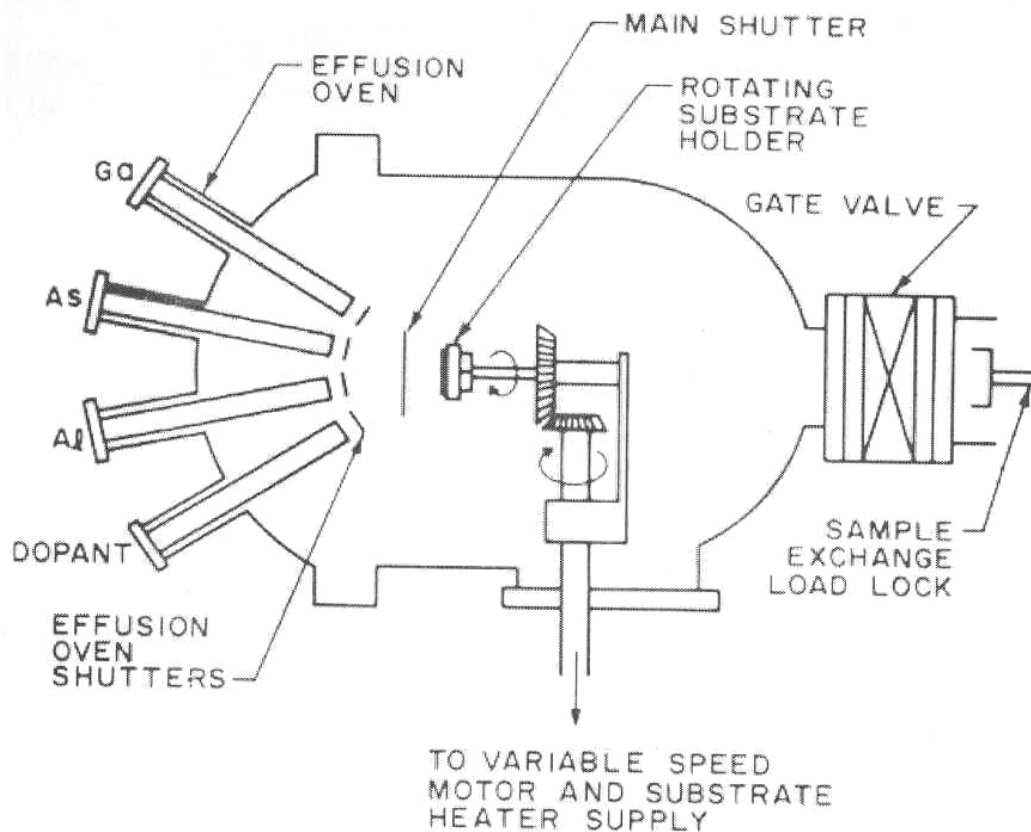
Figure 8. Typical set up of MBE.

MBE also takes place under high vacuum conditions. A better vacuum means less chance for unwanted impurities to enter into the crystal. Vacuum quality is important for $Al_xGa_{1-x}N$ because aluminum's reactivity dictates an oxygen free environment. To keep the pressure under 10^{-11} Torr, cyropanels are used. The substrate is placed in the growth chamber by a load lock. The sample is placed on a rotating holder. This is known as a Continual Azimuthal Rotation (CAR) to ensure that the chemical composition throughout the crystal is as homogeneous as possible.

Crystal growth begins as effusion ovens heat the source atoms and they travel in a straight line, past the open effusion oven shutters, until they collide with the substrate.

16

When one monolayer of source atoms has been formed, the effusion oven shutter for that specific source atom is shut and the shutter for the second source atom is opened. If the technique of in-stiu doping was used while all of this was going on, a dopant, like silicon, would have traveled from an effusion oven into the crystal. Crystal growth goes on at the rate of about 10 monolayers per minute until the crystal is fully grown. Then it is removed from the growth chamber by the same load lock that placed the substrate in the chamber.

2.6 Ion Implantation

The setup of a typical ion implantation device is seen [8:19] in Figure 9. The first step in ion implantation is to ionize the dopant. Secondly, the ions are accelerated to a given energy; for this research the energy is 200 keV. Then the high energy ions are colluminated into a beam using vertical and horizontal scanners. The beam is directed at a specific point on the $Al_xGa_{1-x}N$.
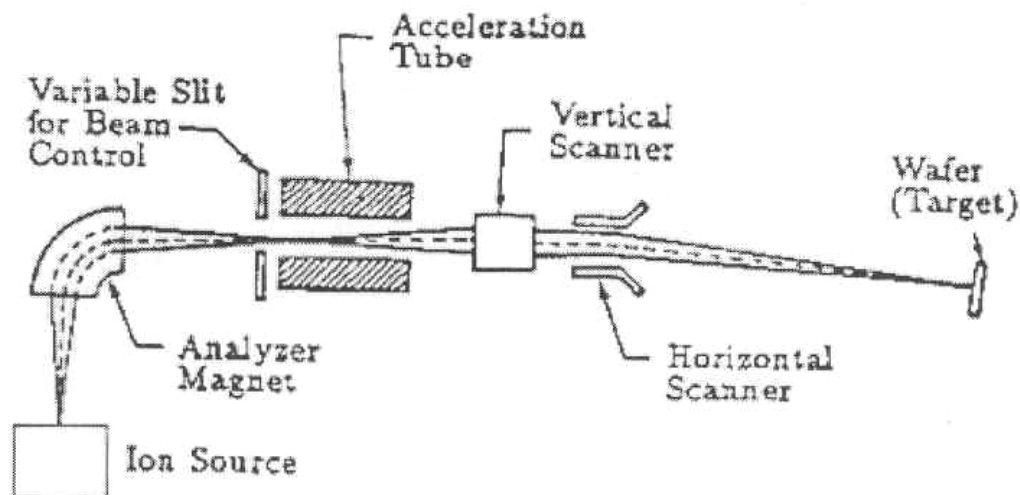
Figure 9. Typical set up of ion implantation device.

The three major methods of placing a dopant into a crystal are ion implantation, diffusion, and in-situ doping. The technique of doping via diffusion is an unfavorable technique because of the properties of $Al_xGa_{1-x}N$. Diffusion doping involves heating a crystal coated with a dopant and letting the dopant diffuse into the crystal. The temperatures required to dope $Al_xGa_{1-x}N$ via diffusion doping are cost and time prohibitive due to the robust chemical composition of $Al_xGa_{1-x}N$. In-stiu doping also requires that MBE takes place at very high temperature, and this can drive up costs and interfere with good crystal growth.

Ion implantation is cheaper, faster, more flexible and generally better suited for $Al_xGa_{1-x}N$ than the methods of diffusion doping and in-stiu doping. Ion implantation is cheaper because it does not require the high temperatures used in diffusion doping and in-stiu doping. Ion implantation is faster because instead of the long process of diffusing dopant into the crystal or placing dopant in the layers of a growing semiconductor, the ions are shot almost instantly into the crystal.

Ion implantation is also more flexible. Using a mask, it is possible to dope a semiconductor with several different levels of impurities on one wafer. Also, it is easy to reproduce the process of implantation; as long as the implantation temperature and implantation energy are the same, subsequent samples will implant in the same way. There is also precise dopant control; there is usually less than 1% error in the measured amount of dopant implanted.

However, ion implantation has its drawbacks as well, the largest of which is radiation damage and to a lesser extent doping depth issues. When a dopant, like silicon,

18

is about to collide with a crystal, it will be slowed down by two types of forces: coulomb repulsion from electrons (electric stopping) and the atomic strong force from the atomic nucleus (nuclear stopping). As could be deduced from the nature of the forces, electric stopping is small in magnitude but wide in range. Conversely, nuclear stopping is strong but does not occur until the silicon atom gets fairly close to a lattice position. When silicon is slowed down due to nuclear stopping, it will often knock an atom out of the lattice leaving a point defect. Point defects -- when clustered together-- form extended defects.

Extended defects are very similar to the shifting caused by crystal and substrate mismatch. The degree to which ion implantation causes extended defects in the crystal depends on the energy and mass of the implanted ion. This is because the greater the mass and energy the more nuclear stopping will occur and the more point impurities will be created in the crystal. The effects of using heavier ions for doping can be seen [17:37] in Figure 10. The degree of extended defects is also related to the crystal into which the ions are implanted. Typically, if the crystal is more ionic there will be less extended defects.
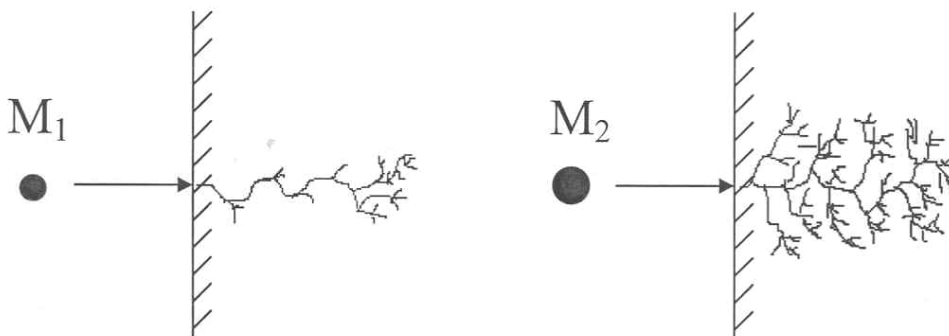
Figure 10. How damage created by ion implantation is related to the mass of the implanted atom, where M1 is the less massive atom

19

The second drawback to ion implantation is that ion implantation only dopes the surface of a crystal. As can be seen [17:33] in Figure 11, the ion dosage for 200 keV silicon ions implanted into GaN is a Gaussian distribution centered at 0.16 µm. It is possible to place ions deeper into the crystal, however, that requires more energy, and more energy creates more extended defects. After ion implantation, the crystal becomes slightly amorphous and it is necessary to anneal out extended defects.
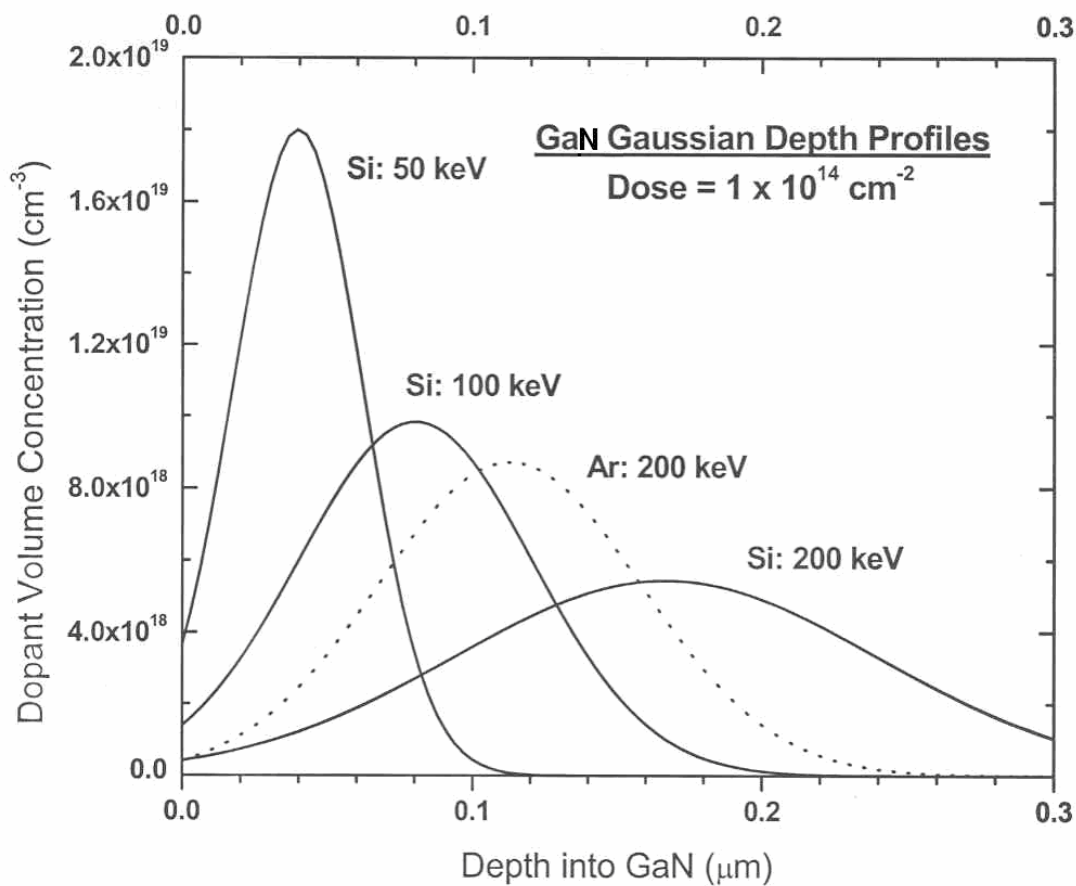
Figure 11. Ion implantation depth profile for silicon implanted into GaN at various energies.

2.7 Annealing

Annealing is the process of restoring the order of a crystal and electrically activating implanted ions. Annealing removes defects in the crystal structure. These defects trap free charge carriers from the dopant. There are two types of annealing used to repair radiation damage in group III-nitrides, rapid thermal annealing (RTA) and conventional furnace annealing (CFA). This research uses the RTA method for the formation of ohmic contacts to the crystal. In RTA the rate at which the anneal chamber is heated is greater than 50 °C per second and the time the crystal spends at this temperature is usually less than 60 s. It is necessary to use the Oxy-Gon annealing system to anneal the damaged crystal because this CFA system can maintain temperatures up to 1700 °C for long periods of time.

If annealing is not done carefully, it can cause more damage than ion implantation. The first danger is that the dopant will diffuse out of the crystal. Group III-V materials are especially vulnerable to out-diffusion. An epitaxially-grown encapsulant is grown to prevent silicon from leaving the crystal. This encapsulant must have certain properties. It must not react chemically with the crystal or the dopant; it must have a coefficient of thermal expansion similar to the crystal; and also must be easily removed. In this research an AlN encapsulant is used. Another technique used to prevent the out diffusion is proximity cap annealing. In this process two semiconductors are bound together by a tantalum wire with their implanted surfaces facing inward. The second danger for annealing $Al_xGa_{1-x}N$ is that the nitrogen will disassociate from the crystal. The encapsulant and proximity cap annealing helps prevent this to some degree. However until multiple identical anneals are preformed, specific survival rates will

21

remain unknown. In addition, during annealing the chamber is filled with ultra high

purity nitrogen gas.

2.8 Hall Effect Theory

This research uses the Hall effect to obtain the electric activation efficiency. The

van der Pauw setup for a Hall effect measurement is shown [17:47] in Figure 12. In a

Hall effect measurement, a semiconductor is placed orthogonal to a magnetic field.

Current is run across the semiconductor using the ohmic contacts. This current moves

electrons across the semiconductor, and holes move in the opposite direction.
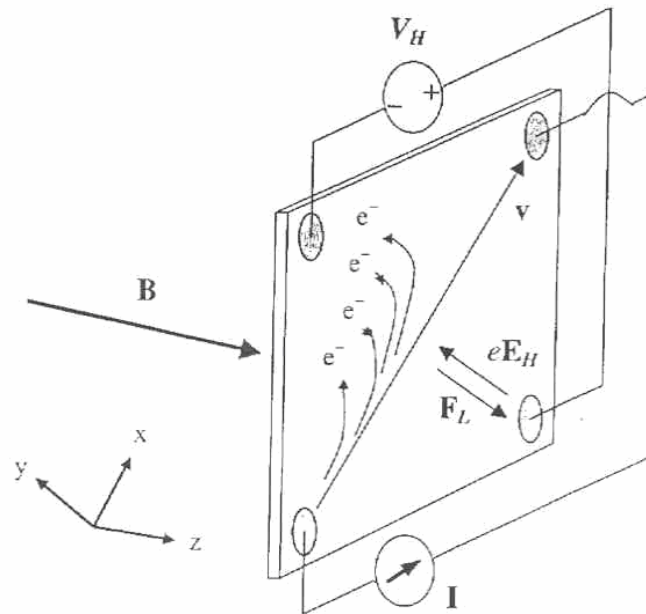
Figure 12. The path of the electrons, the current, the magnetic field, and the
resulting Hall voltage associated with the Hall effect.

Now that the holes and electrons have some velocity they a subject to a Lorentz

force given by Equation-9

22

$$\vec{F}_L = q(\vec{v} \times \vec{B}) , \tag{9}$$

where q is the fundamental charge on the hole or electron, v is the velocity of the charge carrier, and B is the applied magnetic field.

Since the charge carriers have opposite charge and travel in opposite directions, the Lorentz force on all charge carriers will be in the same direction. If there is a clear majority of one type of carrier, a Hall voltage will be produced. From the Hall voltage the sheet Hall coefficient can be obtained using Equation -(10) which states:

$$V_H = \frac{I_x B_z r_H}{e n_s} = R_{Hs} I_x B_z r_H , \tag{10}$$

where I_x is the current applied to the sample, B_z is the magnetic field perpendicular to the sample, r_H is the Hall factor, n_s is the sheet carrier concentration, and R_{Hs} is the sheet Hall coefficient. The volume carrier concentration, n, and Hall coefficient, R_H, can be obtained by the following equations:

$$n = n_s / t \tag{11}$$

and
$$R_H = t \cdot R_{Hs} , \tag{12}$$

where t is a conducting layer thickness of the sample.

23

III. Experimental Procedures

3.1 Sample Growth

The $Al_xGa_{1-x}N$ used in this research was grown by SVT Technology. Using MBE, one micron of $Al_xGa_{1-x}N$ was grown on sapphire substrates with a 200 Å buffer layer of AlN. The AlN is chosen as the buffer layer because its lattice constant is a closer match to $Al_xGa_{1-x}N$ than sapphire. This minimizes dislocation lines in the crystal. The backside of the substrate was coated with titanium to ensure even heating during the growth process. The $Al_xGa_{1-x}N$ was grown at a rate of 1 μm per hour. During the growth process, reflection high-energy electron diffraction was used to monitor the growth quality.

3.2 Preparation and Ion Implantation

Ion implantation is the desired method for introducing dopants into the semiconductor material. This process is chosen for its precise control over the dopant depth profile and its ability of selective area doping. The implantation took place at room temperature. The implantation energy was 200 keV, and low ion doses were investigated. To prepare the wafer for ion implantation, the titanium layer was removed using a hydrofluoric acid bath. Then the samples were cut in four quarters using a wafer saw at Air Force Research Laboratory (AFRL). Three quarters of the 2 inch wafer were doped with silicon at three different ion doses, $1x10^{13}$, $5x10^{13}$, and $1x10^{14}$ cm^{-2}. The samples were implanted by Implant Sciences Corporation. One quarter of the wafer was left unimplanted as a control sample. The silicon-implanted wafers are then divided into

24

5 mm squares using a wafer saw operated by AFRL. The location of each square as it relates to the original wafer is noted. Each sample is cleaned using acetone, methanol, and deionized water. The samples were then blown dry with N_2. In this study two different $Al_xGa_{1-x}N$ wafers were used one having an aluminum mole fraction of 0.1 and the other one having an aluminum mole fraction of 0.2.

3.3 Annealing

Annealing is a necessary step in repairing the damage to the crystal structure caused by ion implantation and also in activating the implanted ions. The annealing time and temperature was varied in order to determine the optimum conditions for each material.

Prior to annealing, the AlN-capped $Al_xGa_{1-x}N$ samples were inscribed with a distinguishing mark on the backside, cleaned again, and tightly wrapped face to face using 5 mm-thick Ta-wire to provide extra protection from any dopant diffusion and nitrogen dissociation during annealing. An Oxy-Gon annealing furnace was used to anneal samples at temperatures from 1100 to 1350 ^{o}C for times of 20 to 40 minutes in an ultra high purity nitrogen environment. A graph of the relationship between temperature of the sample and oven with respect to time is shown [8:31] in Figure 13.

25
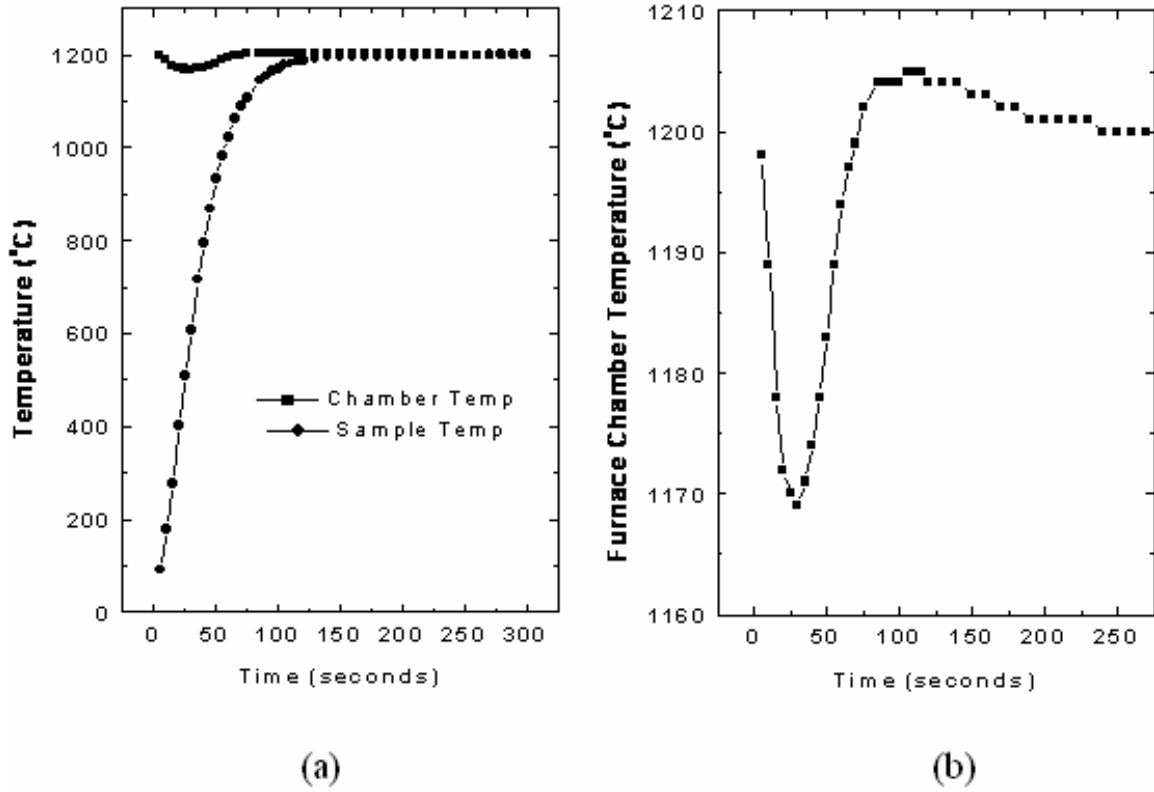
Figure 13. Temperature comparison of the Oxy-Gon furnace and sample
temperatures (a) the furnace alone (b) as a function of time.

Figure 13 (b) shows a dip in temperature this is due to the sample being loaded

into the furnace chamber. The temperatures were measured using two thermocouples.

One thermocouple was place inside the furnace and the other was placed on the sample

mount. When the sample is loaded into the chamber and the isolation value is closed

time is zero.

3.4 Ohmic contacts

The formation of high quality ohmic contacts that have low contact resistivity and

high light transmittance is important for further refinement of electrical and optical

26

devices. Surface treatments are often employed to remove a layer of contamination between the sample surfaces and the contact metal.

Ohmic contacts are required for taking electrical measurements. Prior to metallization, the AlN cap layer was selectively removed by etching for 10 minutes in a solution of 0.5 M KOH at 95 °C, after which the samples were rinsed in deionized water (DI) and immediately placed in boiling aqua regia (3:1, HCl:HNO$_3$) for 2 minutes. The samples were then removed from the acid, rinsed in DI, and blown dry with N$_2$. The annealed samples were examined with an optical microscope.. The samples are then place on a van der Pauw shadow mask in preparation for electron-beam evaporation. The metal is deposited under vacuum pressure of 10^{-6} Torr. The contacts used in this study consisted of a base layer of 300 Å of titanium followed by 800 Å of aluminum, 1200 Å of titanium and a final 550 Å thick layer of gold. The sample is allowed to cool for 30 minutes before it is removed from the electron-beam evaporator which is under vacuum. Following the metal deposition, the samples are annealed in a nitrogen environment at 900 ºC for 45 seconds using a rapid thermal annealing (RTA) system. The ohmicity of the contacts is then inspected using a voltage current probe.

3.5 Hall effect measurements

The Hall coefficient, R_H, and sheet resitivity, ρ_s, measurements are taken using the van der Pauw technique. This technique is advantageous because it does not require that the ohmic contacts form a perfect square, only that they be on the perimeter of the sample. Eight measurements of voltage and current are averaged to calculate the sheet resitivity. Four measurements of voltage and current, taken under forward and reverse magnetic fields are averaged to get the Hall coefficient. The sheet resitivity and the Hall

27

coefficient are used to calculate sheet carrier concentration and Hall mobility using the following equations:

$$N_s = \frac{r_H}{q \cdot R_H}$$
(13)

and
$$\mu_H = \frac{R_H}{\rho_s} \, ,$$
(14)

where q is the elementary charge and r_H is the Hall factor, which although it sometimes ranges from one to two, is taken to be unity. Using the sheet carrier concentration, the activation efficiency is calculated in the following manner:

$$A = \frac{N_s}{D}$$
(15)

where A is the activation efficiency, and D is the effective implantation dose.

The measurements of sheet resistivity, mobility, and sheet carrier concentration are taken four times and if the measurements are within 4% of each other, the data is used. The set up of the Hall measurement system is shown in Figure 14.

28
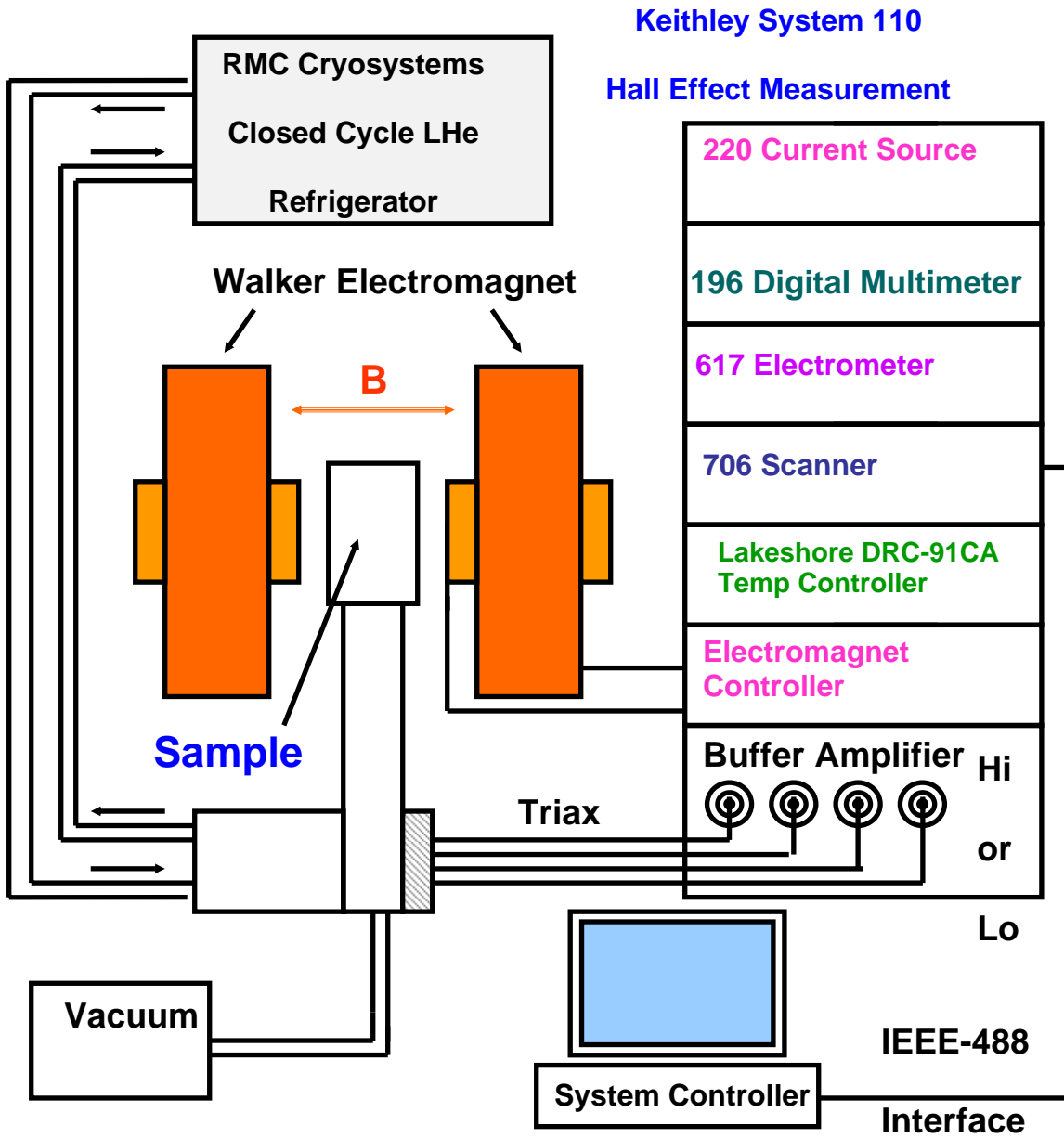
Figure 14. Setup of the Hall Measurement system.

4.1 Room Temperature Hall Measurements of $Al_{0.1}Ga_{0.9}N$

The $Al_{0.1}Ga_{0.9}N$ samples were implanted with 3 different silicon ion doses of $1x10^{13}$, $5x10^{13}$, and $1x10^{14}$ cm^{-2} at room temperature and at 200 keV. The samples were annealed at four different temperatures of 1100, 1150, 1200, and 1250 ºC for 20 minutes. The samples were annealed in the Oxy-Gon anneal system. The Hall coefficient and resistivity were measured using room temperature Hall effect measurements. From this data the Hall mobility, sheet carrier concentration, and electrical activation efficiencies were calculated.

The samples annealed at 1150 and 1200 ºC displayed minor damage, less than 10%, on the surface. However, the control sample and the sample implanted annealed at 1250 ºC for 20 minutes with $1x10^{13}$ cm^{-2} silicon showed extreme damage, about 60 % surface damage, indicating a complete destruction of the AlN cap. The damage was so extensive that ohmic contacts could not be placed on these samples. The liquid gallium on the surface signifies nitrogen dissociation. The results of Hall effect and sheet resistivity measurements made on the implanted $Al_{0.1}Ga_{0.9}N$ samples are shown in Figure 15.

In Figure 15, the carrier concentrations of the $Al_{0.1}Ga_{0.9}N$ have had the background carrier concentration subtracted out of the measured carrier concentration. The subtracted background carrier concentrations are shown in Figure 15.
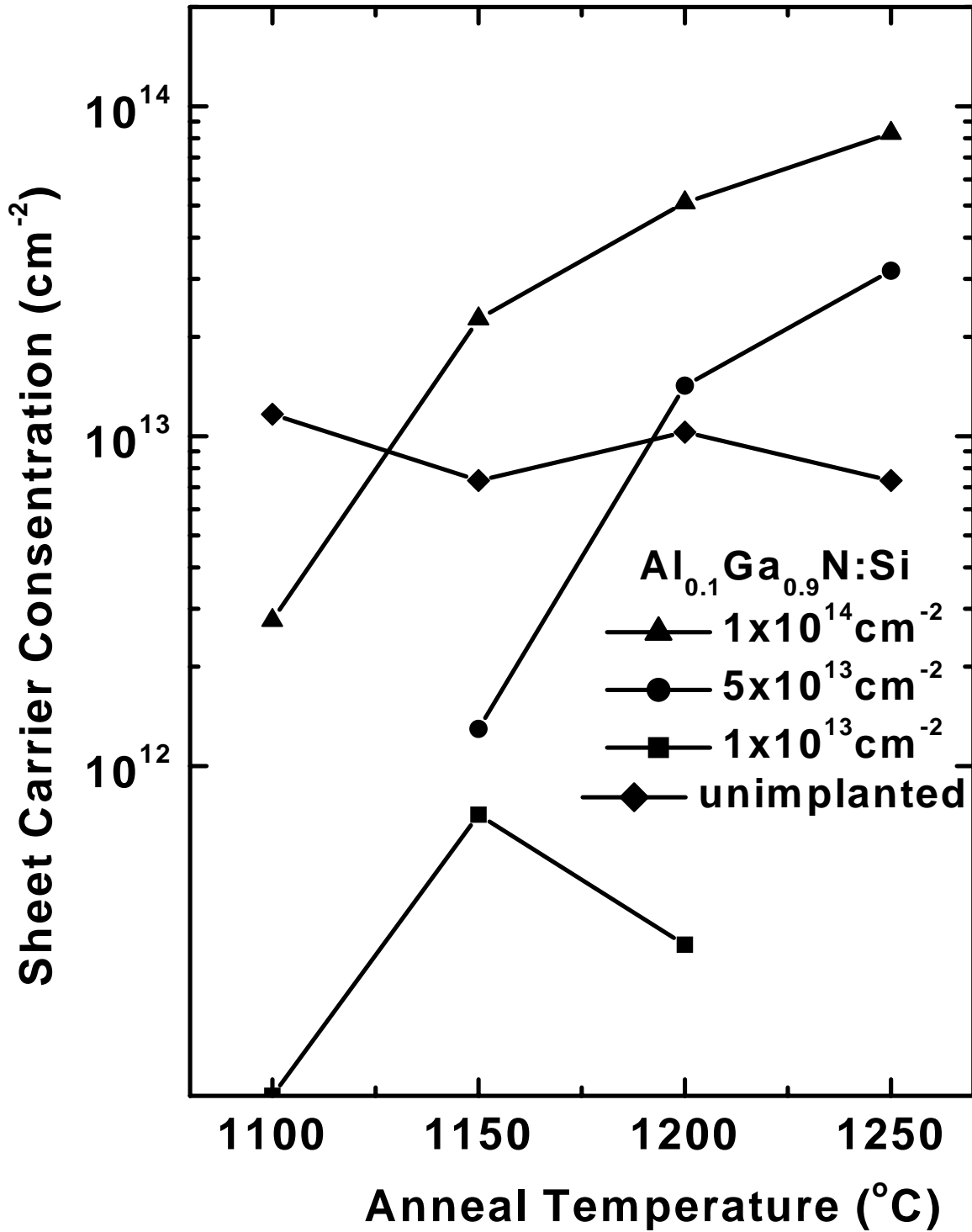
Figure 15. Room temperature sheet carrier concentration of implanted silicon in Al$_{0.1}$Ga$_{0.9}$N annealed for 20 minutes as a function of anneal temperature .

31
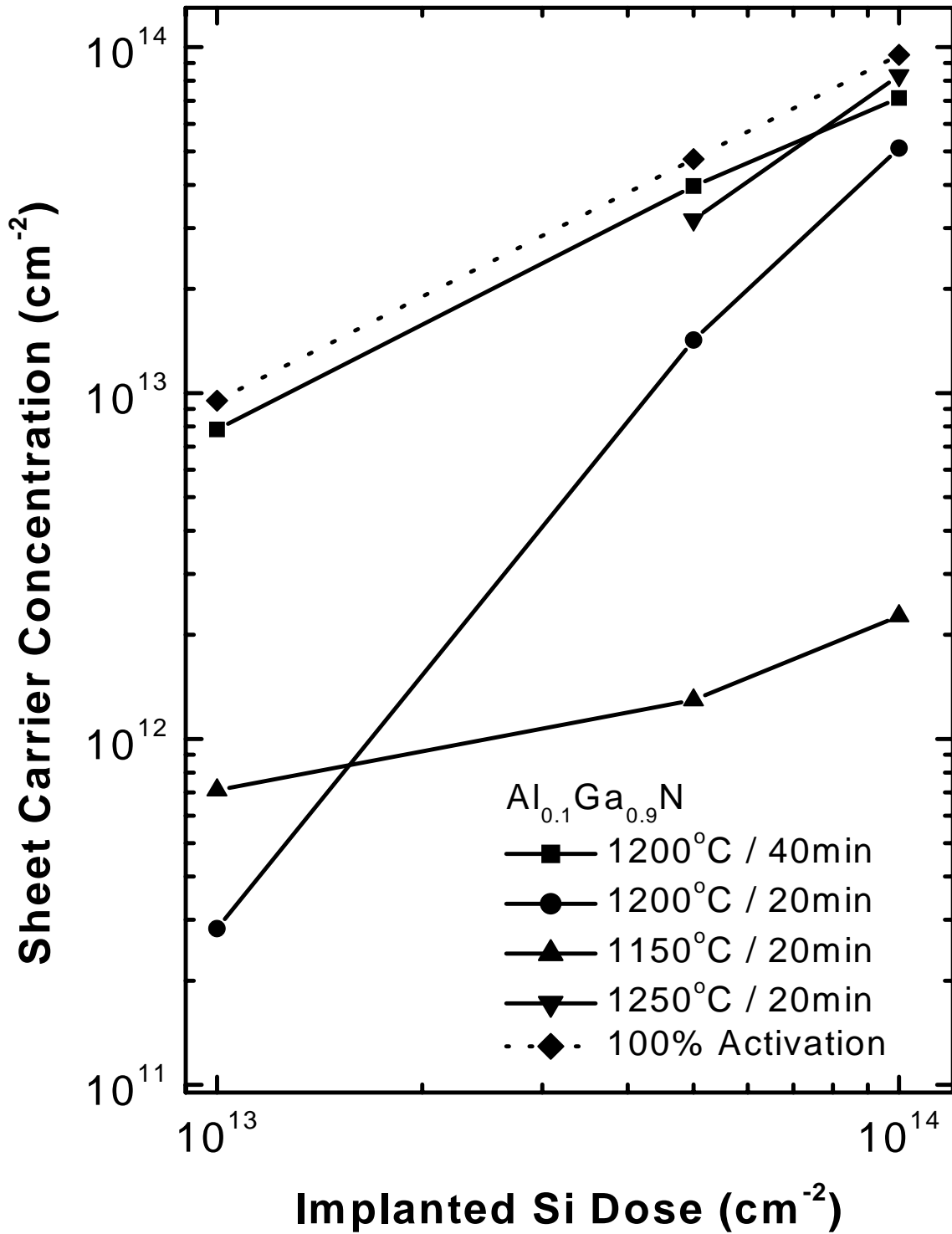
Figure 16. Room temperature sheet carrier concentration of implanted silicon in $Al_{0.1}Ga_{0.9}N$ as a function of implanted ion dose.

The background concentration comes from unimplanted samples that are annealed at 1100, 1150, 1200, 1250 ℃ for 20 minutes. The average back ground sheet carrier concentration was 9.8×10^{12} cm^{-2}.

Figure 15 shows that as anneal temperature increased all samples showed higher sheet carrier concentrations. The highest sheet carrier concentration of 8.28×10^{13} cm^{-2} was obtained from the sample implanted with 1×10^{14} cm^{-2} silicon ions and annealed at 1250 ℃ for 20 minutes. At the same temperature and for the same time, the sample implanted with 5×10^{13} cm^{-2} silicon ions showed a sheet carrier concentration of 3.17×10^{13} cm^{-2}. The sample implanted with 1×10^{13} cm^{-2} silicon ions showed very low sheet carrier concentration when annealed for 20 minutes at 1100, 1150, 1200, and 1250 ℃. The sample showed only 7×10^{11} to 2×10^{11} cm^{-2} above the background sheet carrier concentration. The sheet carrier concentration is a function of implanted silicon and anneal temperature. The relation between implantation dose and sheet carrier concentration is shown in Figure 16.

The Hall mobilities of the implanted Al$_{0.1}$Ga$_{0.9}$N samples are shown in Figure 17. The highest mobilities of 89 cm^2/V·s were obtained by the Al$_{0.1}$Ga$_{0.9}$N samples implanted with both 1×10^{14} and 5×10^{13} cm^{-2} silicon. As the anneal temperature is increased, the mobilities of all samples increased. The values for mobility range from 4.3 to 89.3 cm^2/V·s.

The electrical activation efficiencies of the implanted silicon in the Al$_{0.1}$Ga$_{0.9}$N samples are shown in Figure 18. The highest activation efficiencies for the 1×10^{14} and 5×10^{13} cm^{-2} silicon implanted samples were 87.2 and 66.8%, respectively, achieved by annealing at 1250 ℃ for 20 minutes.
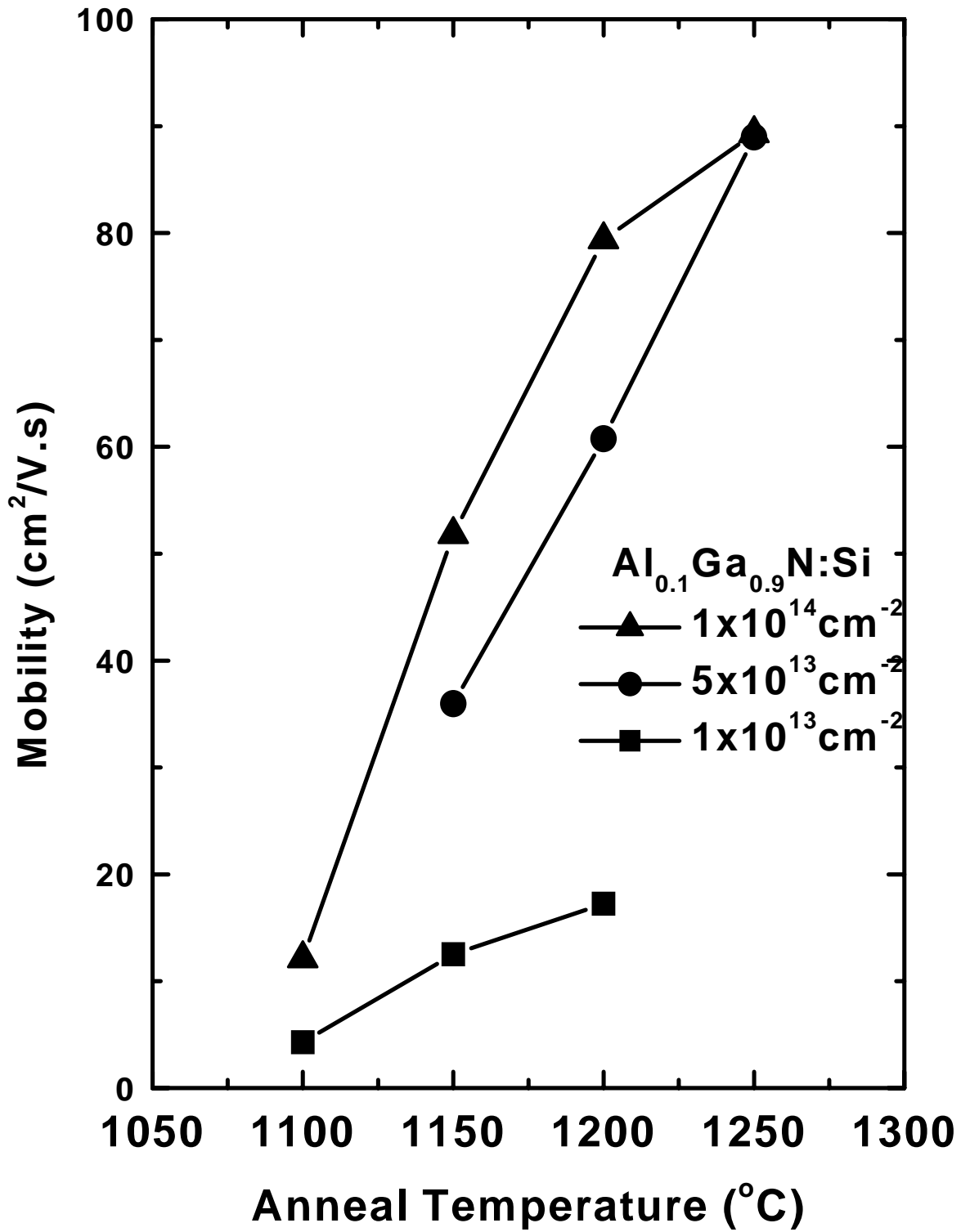
Figure 17. Room temperature Hall mobility of $Al_{0.1}Ga_{0.9}N$ annealed for 20 minutes as a function of anneal temperature .

34
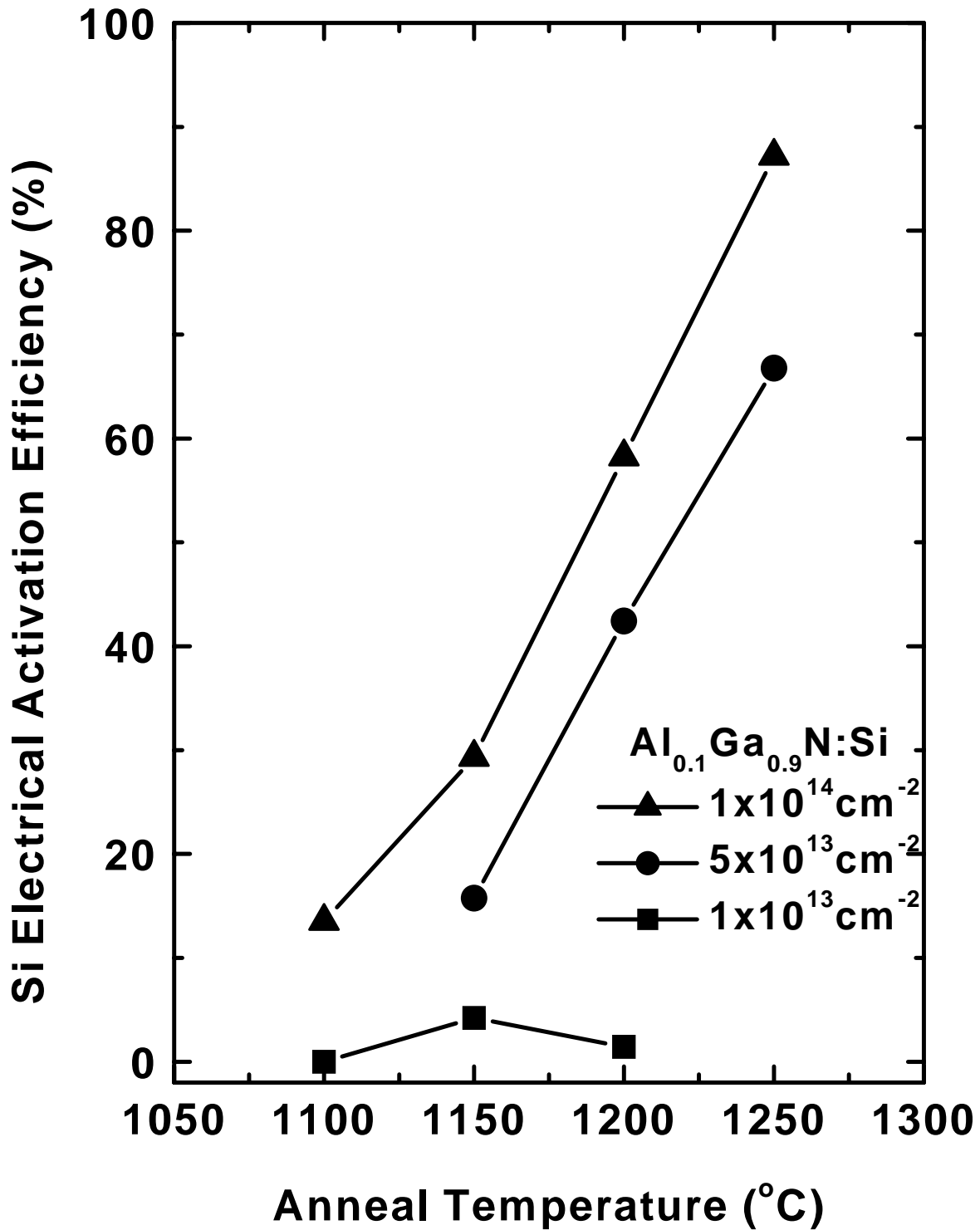
Figure 18. Room temperature electrical activation efficiency of implanted silicon in $Al_{0.1}Ga_{0.9}N$ annealed for 20 minutes as a function of anneal temperature .

The damage caused at 1250 ºC to the control sample and the sample implanted with $1x10^{13}$ cm^{-2} silicon was great, over 50% surface damage, due to damage to the AlN cap. Moreover, 1250 ºC is not a commercially viable temperature for the fabrication of semiconductor devices. Therefore 1200 ºC was chosen as the temperature for anneal time dependent Hall measurements. The $Al_{0.1}Ga_{0.9}N$ samples implanted with 3 different silicon ion doses of $1x10^{13}$, $5x10^{13}$, and $1x10^{14}$ cm^{-2} at room temperature at 200 keV were annealed at 1200 ºC for 30 and 40 minutes. The samples were annealed in the Oxy-Gon anneal system. Hall measurement data from the previous anneal at 1200 ºC for 20 minutes were used to find optimum anneal time.

The samples annealed for 20 minutes showed some minor signs of damage in the form of small gallium bubbles on the sample surface. When anneal time was increased to 30 minutes, the number of gallium bubbles remained comparable. Finally, at an anneal time of 40 minutes, although the number of gallium bubbles did not change a great deal they were larger and covered more surface area. The minor damage due to nitrogen dissociation in the samples annealed at 1200 ºC for 20 minutes did not prevent the samples from forming good ohmic contacts. The results of Hall effect and sheet resistivity measurements made on the implanted $Al_{0.1}Ga_{0.9}N$ samples are shown in Figure 19.

In Figure 19, the carrier concentrations of the $Al_{0.1}Ga_{0.9}N$ samples have had the background carrier concentration subtracted out of the measured carrier concentration. The subtracted background carrier concentrations are shown in Figure 19. The carrier concentration is a function of dopant level and anneal time. In general, as the samples

36
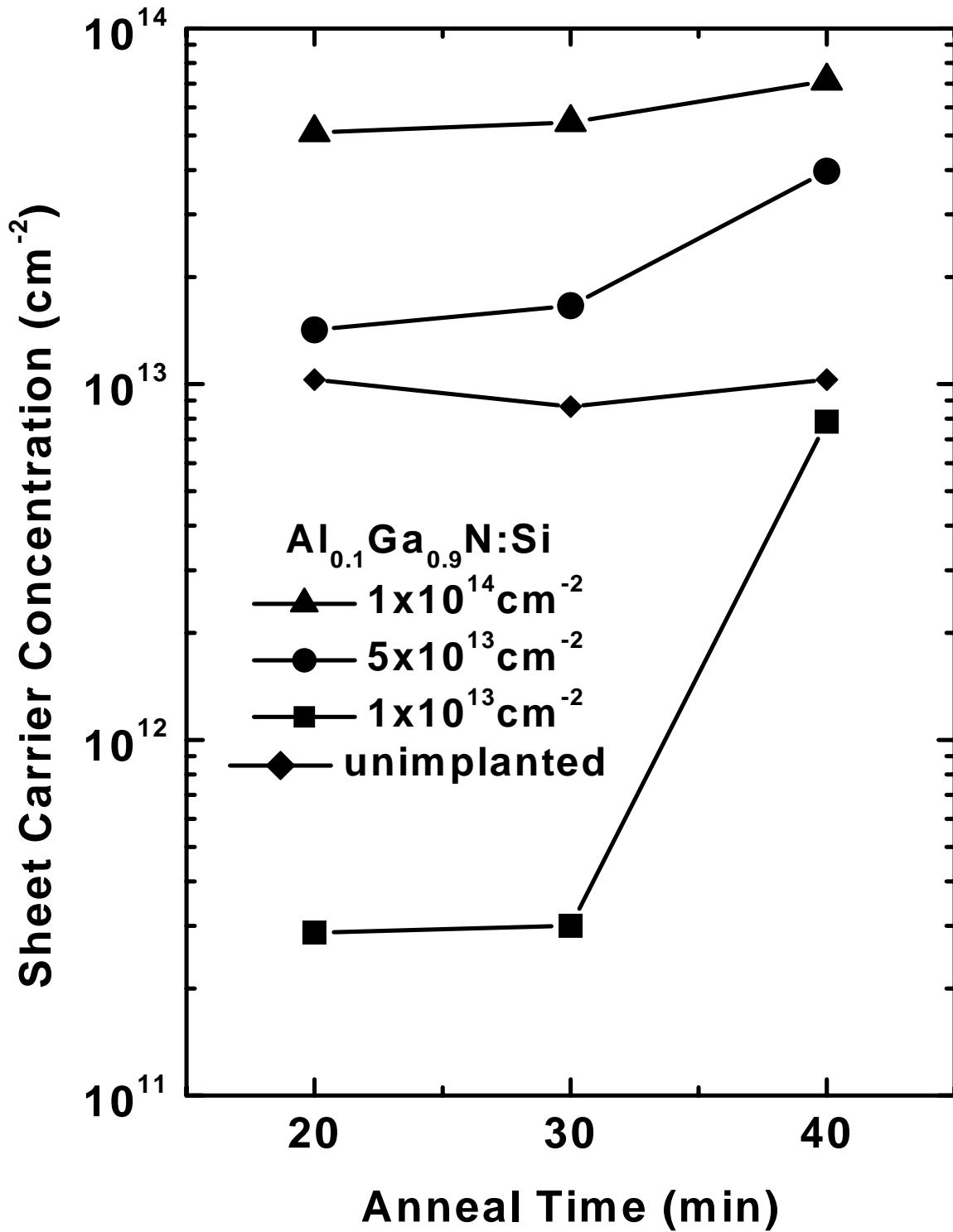
Figure 19. Room temperature sheet carrier concentration of implanted silicon in
Al$_{0.1}$Ga$_{0.9}$N annealed at 1200 °C as a function of anneal time.

www.manaraa.com

were annealed for longer times the samples showed higher sheet carrier concentrations. The highest sheet carrier concentration of 7.13×10^{13} cm^{-2} was obtained from the sample implanted with 1×10^{14} cm^{-2} silicon and annealed for 40 minutes at 1200 ℃. At the same temperature and for the same time the sample implanted with 5×10^{13} cm^{-2} silicon showed a sheet carrier concentration of 3.97×10^{13} cm^{-2}. The sample implanted with 1×10^{13} cm^{-2} silicon showed very low sheet carrier concentration for the anneals of 20 and 30 minute duration. However, at an anneal time of 40 minutes the sheet carrier concentration jumped 7.84×10^{12} cm^{-2} above the background sheet carrier concentration. This is an indication that some crystal damage due to ion implantation was recovered with a longer anneal at 1200 ℃.

The Hall mobilities of the implanted $Al_{0.1}Ga_{0.9}N$ samples are shown in Figure 20. The highest mobilities of 89.0 and 88.1 cm^2/V·s were obtained by the $Al_{0.1}Ga_{0.9}N$ samples implanted with 5×10^{13} and 1×10^{14} cm^{-2} silicon, respectively. Both samples were annealed for 40 minutes at 1200 ℃. These mobilities are almost identical to the same results achieved by annealing $Al_{0.1}Ga_{0.9}N$ samples at 1250 ℃ for 20 minutes. As the anneal time is increased, the mobility of all samples increase. The values for mobility ranged from 17.6 to 89.0 cm^2/V·s. The mobility of a sample implanted with 1×10^{13} cm^{-2} silicon increased to 34.6 cm^2/V·s above when annealed at 1200 ℃ for 40 minutes, indicating a recovery of implantation damage.

The electrical activation efficiencies of the implanted samples are shown in Figure 21. The efficiencies of the silicon implanted samples are based on the activation of implanted silicon alone and do not include the values of background charge carriers.

38
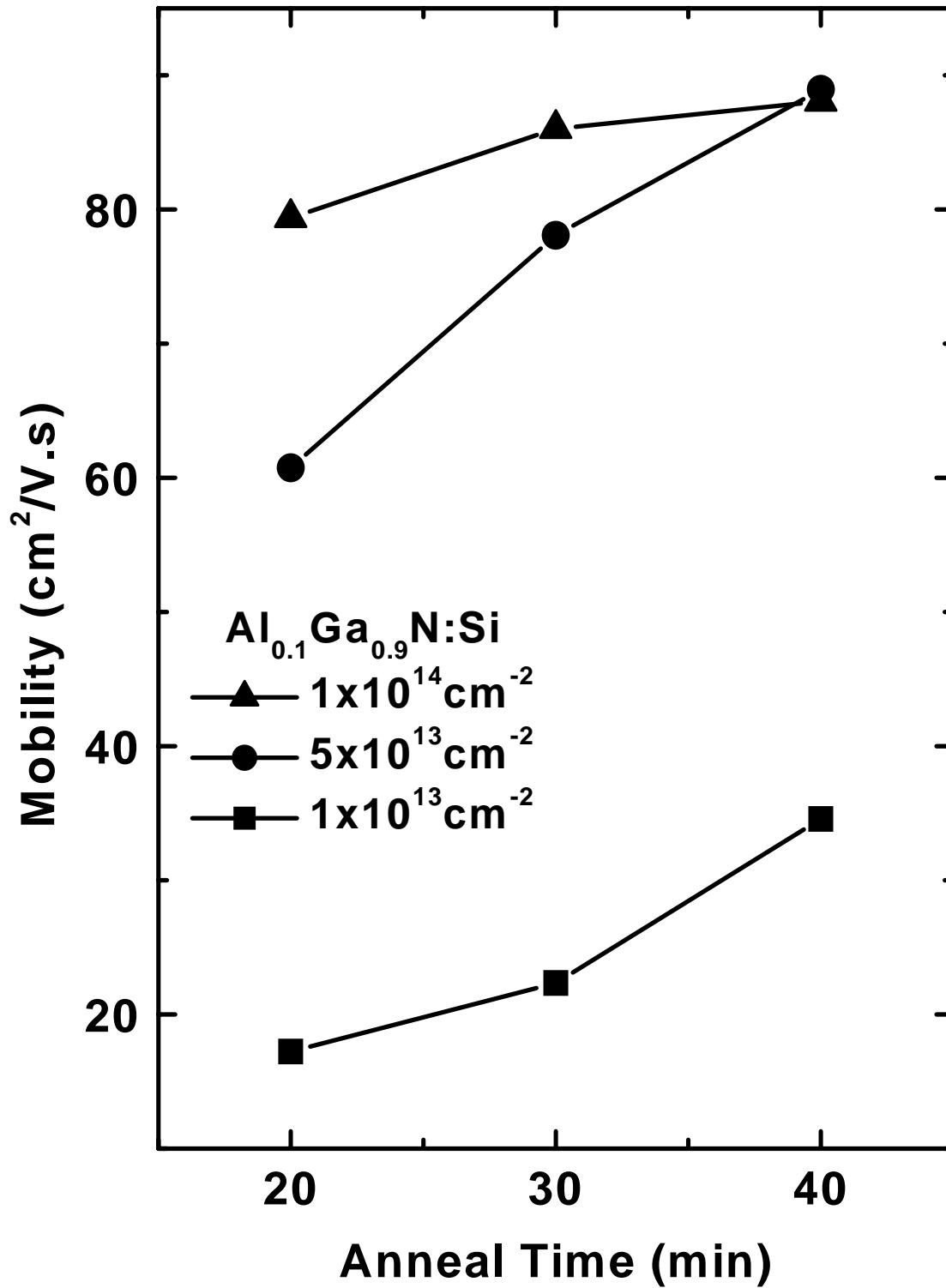
Figure 20. Room temperature Hall mobility in $Al_{0.1}Ga_{0.9}N$ annealed at 1200 °C as a function of anneal time.
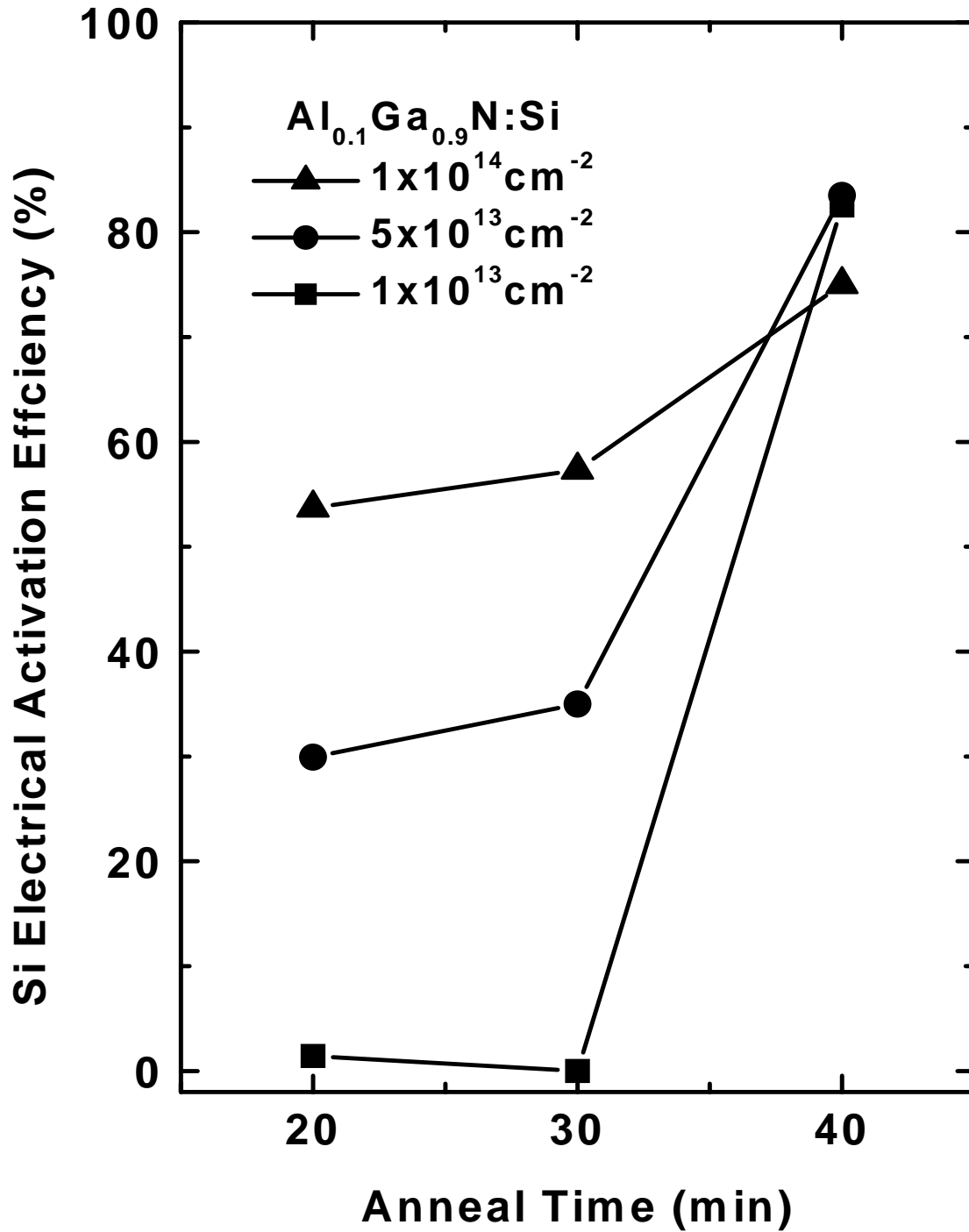
Figure 21. Room temperature electrical activation of implanted silicon in
$Al_{0.1}Ga_{0.9}N$ annealed at 1200 °C as a function of anneal time.

The highest activation efficiencies for the $5x10^{13}$ and $1x10^{13}$ cm^{-2} silicon implanted samples were 83.5 and 82.6%, respectively. This was achieved by annealing at 1200 ℃ for 40 minutes. The peak electrical activation efficiency of the $1x10^{14}$ cm^{-2} sample is 75.0% which is 14.0% less than the efficiency achieved annealing at 1250 ℃ for 20 minutes. However there is a vast improvement in the activation of both the $1x10^{13}$ and $5x10^{13}$ cm^{-2} samples. In all but one of the samples as the anneal time is increased the electrical activation is increased.

4.2 Room Temperature Hall Measurements of Al$_{0.2}$Ga$_{0.8}$N

The Al$_{0.2}$Ga$_{0.8}$N samples were implanted with 3 different silicon ion doses of $1x10^{13}$, $5x10^{13}$, and $1x10^{14}$ cm^{-2} at room temperature with an energy of 200keV. The samples were annealed at five different temperatures of 1150, 1200, 1250, 1300, and 1350 ℃ for 20 minutes. All samples were annealed in the Oxy-Gon anneal system. The Hall coefficient and resistivity were obtained using room temperature Hall effect measurements. From this data the Hall mobility, sheet carrier concentration, and electrical activation efficiencies were calculated

Precautions were taken to ensure that the AlN protective layer survived, but at 1350 ℃ there was noticeable damage to the sample in the form of liquid gallium on the sample surface signifying nitrogen dissociation. There was some minor damage for anneals at 1300 ℃ for 20 minutes, but no damage could be seen by visual inspection for anneals below 1300 ℃.

The sheet carrier concentrations of the silicon ion implanted samples are shown in Figure 22. For all of the samples, the background carrier concentration has been

41
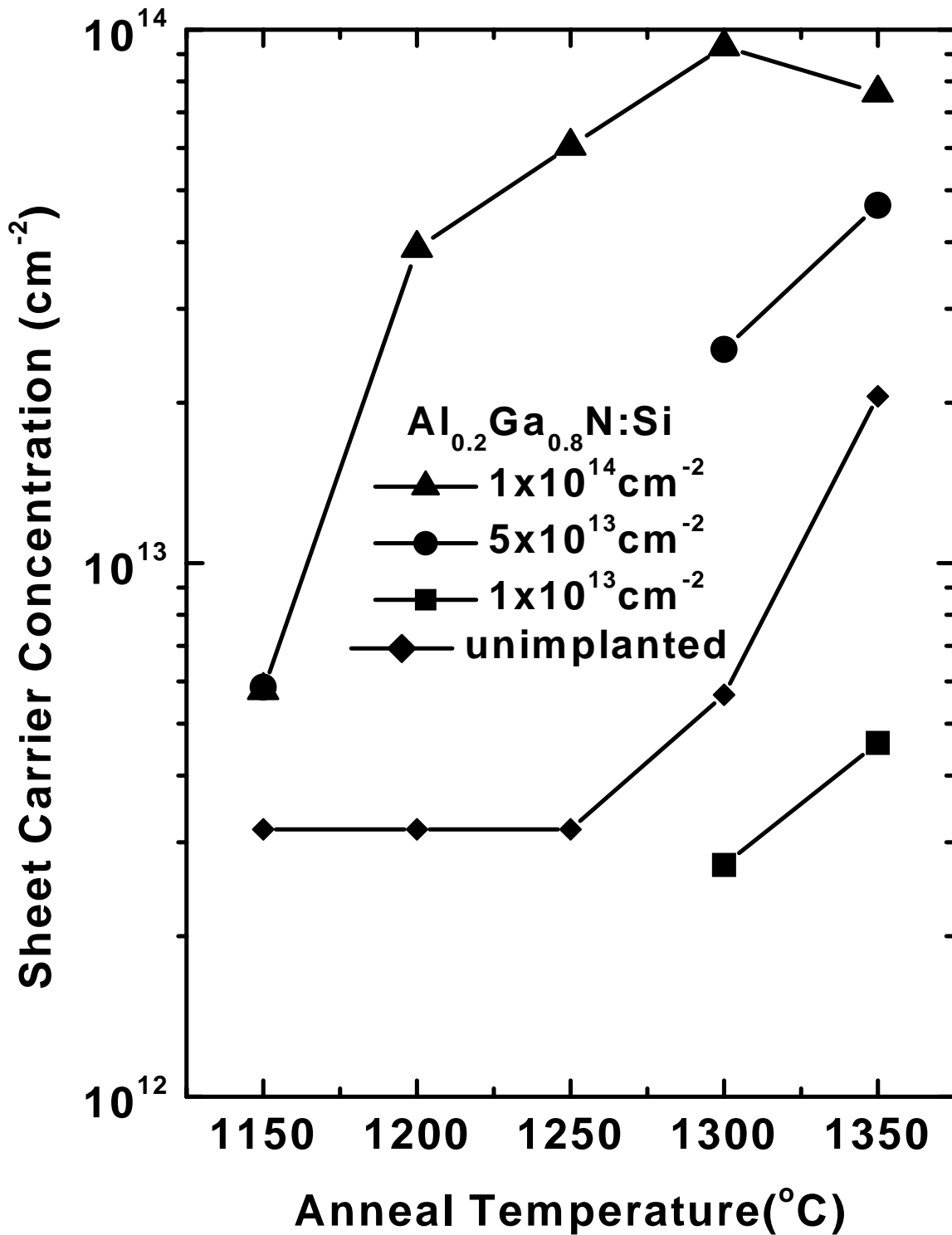
Figure 22. Room temperature sheet carrier concentration of implanted silicon in $Al_{0.2}Ga_{0.8}N$ annealed for 20 minutes as a function of anneal temperature .

subtracted from the measured carrier concentration. The subtracted background carrier concentrations are shown in Figure 22. The average back ground sheet carrier concentration of implanted samples was 9.7×10^{12} cm^{-2}. The sheet carrier concentration is a function of the anneal temperature and the silicon dopant levels. The relation between dopant levels and sheet carrier concentration is shown in Figure 23. As the anneal temperature goes up the sheet carrier concentration increases. However, for the sample doped with 1×10^{14} cm^{-2} silicon, the sheet carrier concentration drops off at 1350 ºC due to excessive nitrogen dissociation. On the other hand, sheet carrier concentration increased as temperature was raised to 1350 ºC for the $Al_{0.2}Ga_{0.8}N$ samples doped with 1×10^{13} and 5×10^{13}cm^{-2} silicon. The highest sheet carrier concentration of 9.28×10^{13}cm^{-2} was obtained for $Al_{0.2}Ga_{0.8}N$ doped with 1×10^{14} cm^{-2} silicon and annealed at 1300 ºC.

The Hall mobilities of the implanted $Al_{0.2}Ga_{0.8}N$ samples are shown in Figure 24. The highest mobility of 75.7 cm^2/V·s was obtained by the $Al_{0.2}Ga_{0.8}N$ sample implanted with 1×10^{14} cm^{-2} silicon and annealed for 20 minutes at 1350 ºC. As the anneal temp is increased the mobilities of all samples increased, up to 1300 ºC. At an anneal temperature of 1300 ºC, the damage due to nitrogen dissociation and the damaged recovery due to annealing vie for dominance. No conclusion can be reached as to the dominant factor without further study. The values for mobility ranged from 6.00 to 75.7 cm^2/V·s.
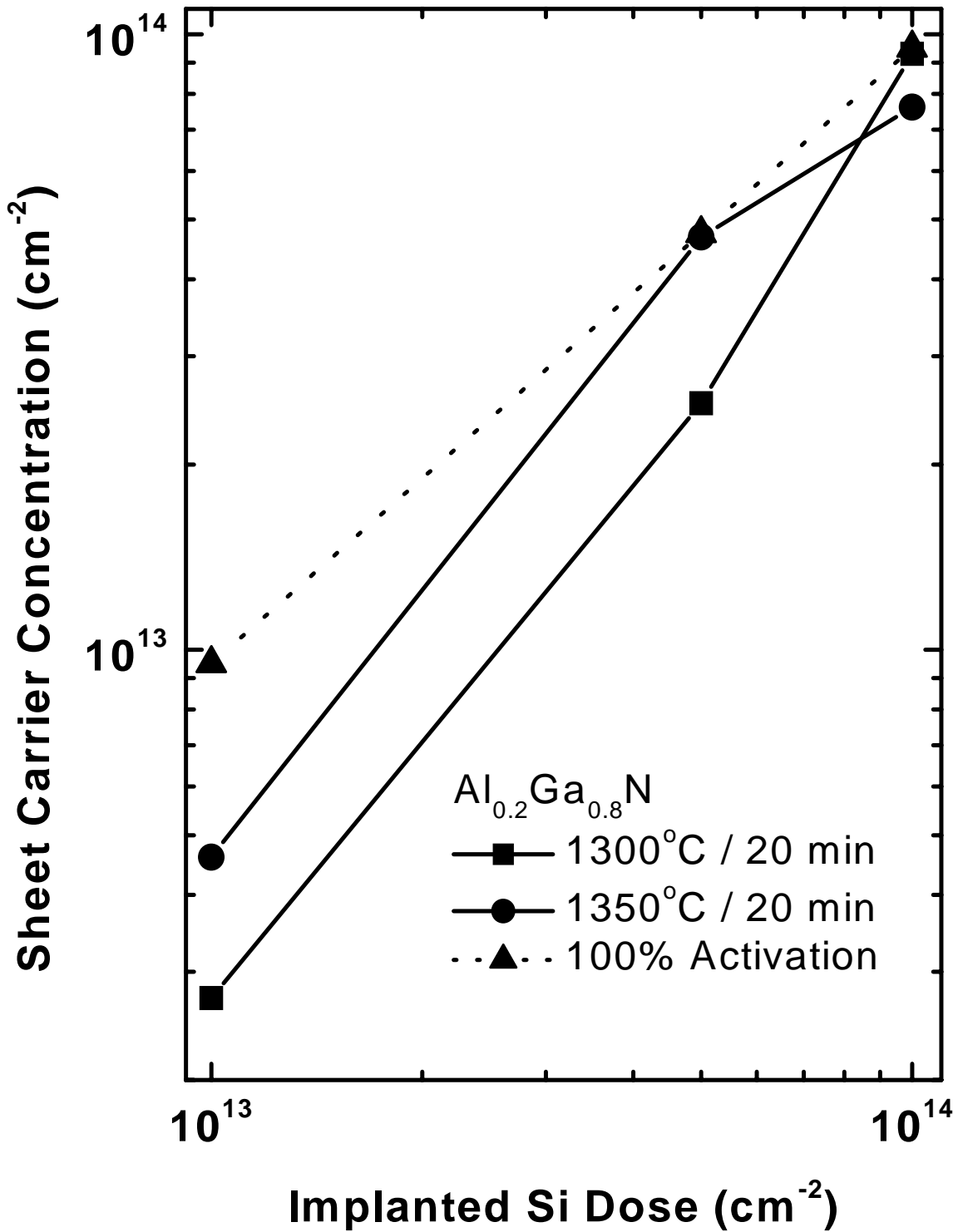
Figure 23. Room temperature sheet carrier concentration of implanted silicon in $Al_{0.2}Ga_{0.8}N$ as a function of implanted ion dose.
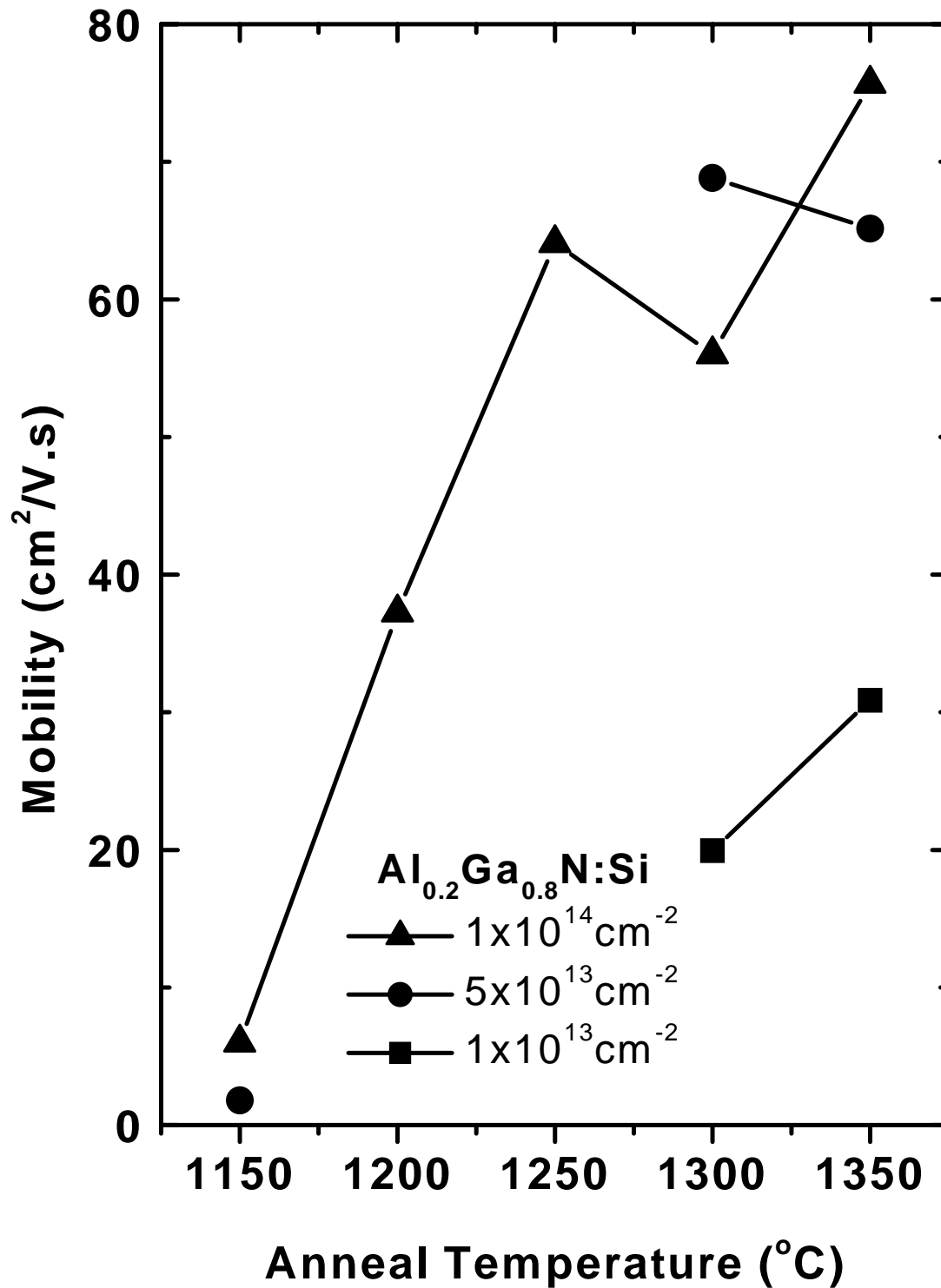
Figure 24. Room temperature Hall mobility in $Al_{0.2}Ga_{0.8}N$ annealed for 20 minutes as a function of anneal temperature .

45
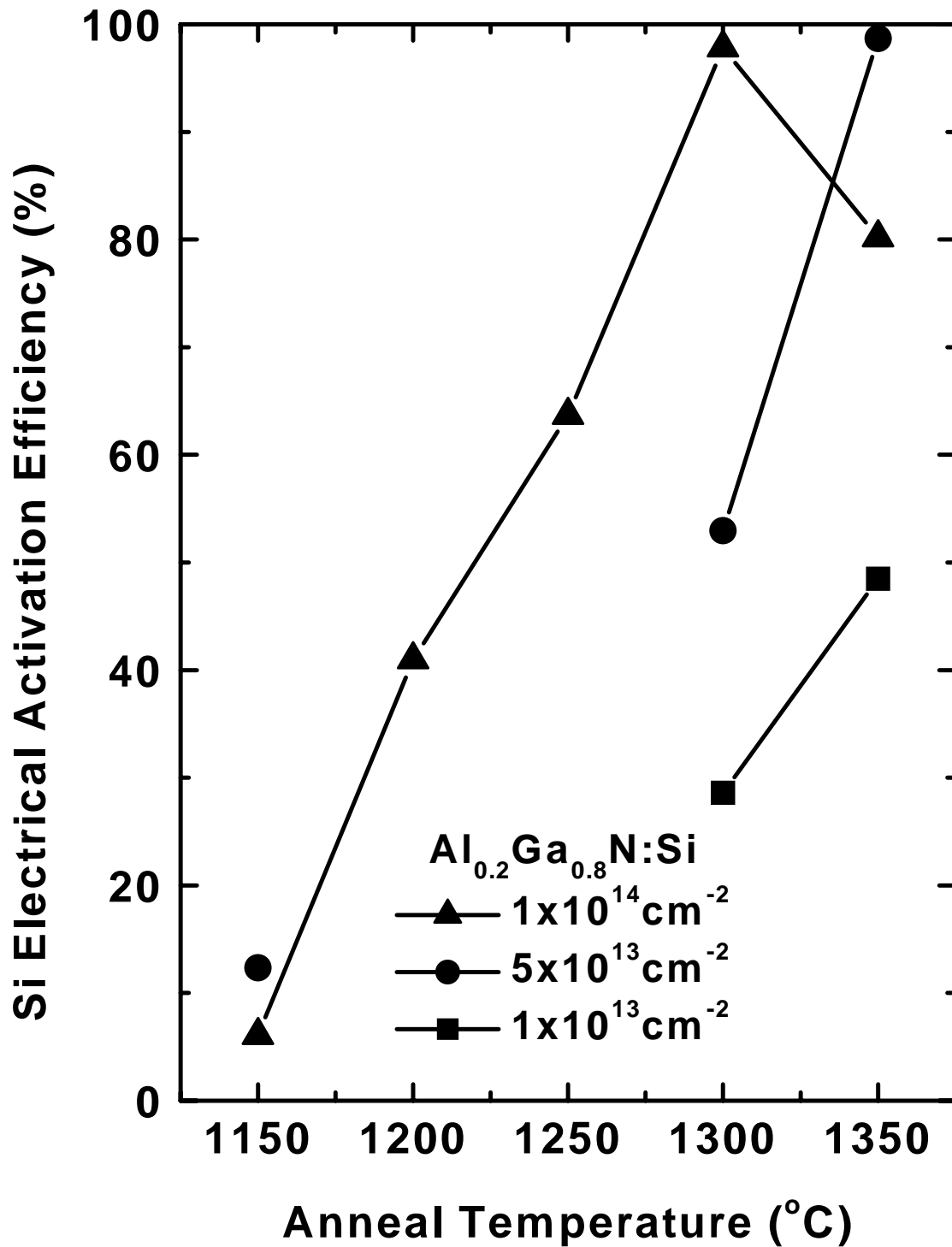
Figure 25. Room temperature electrical activation efficiency of implanted silicon in $Al_{0.2}Ga_{0.8}N$ annealed for 20 minutes as a function of anneal temperature.

The electrical activation efficiencies of the implanted samples are shown in Figure 25. The efficiencies of all the implanted samples are based off of the activation of implanted silicon alone. The highest activation efficiencies for the $1x10^{14}$ and $5x10^{13}$ cm^{-2} silicon implanted samples were 98 and 99%, respectively, which were achieved by annealing at 1300 ºC and 1350 ºC, respectively, for 20 minutes. These activation efficiencies suggest removal of implantation damage. The activation efficiency of the samples was a function of anneal temperature as anneal temperature rose all samples exhibited greater activation efficiency. The $Al_{0.2}Ga_{0.8}N$ sample implanted with $1x10^{13}$ cm^{-2} silicon showed activation efficiencies 24 to 69% lower than the samples implanted with high dopant levels.

The electrical properties of silicon implanted $Al_xGa_{1-x}N$ have been investigated as a function of anneal time, temperature, and ion dose in order to find the optimal annealing conditions for best electrical activation.

$Al_{0.1}Ga_{0.9}N$ wafers, with a 500 Å protective layer of AlN, were implanted at room temperature with silicon ion doses ranging from $1x10^{13}$ to $1x10^{14}\, cm^{-2}$ at an energy of 200 keV. The samples were annealed at temperatures ranging from 1100 to 1250 °C for 20 minutes. The Hall coefficient and resistivity were measured using room temperature Hall effect measurements. From this data the Hall mobility, sheet carrier concentration, and electrical activation efficiencies were calculated. A second set of $Al_{0.1}Ga_{0.9}N$ samples were annealed at 1200 °C for 30 and 40 minutes and their electrical properties were assessed.

This research found that as anneal temperature was increased Hall mobility, sheet carrier concentration, and electrical activation efficiency were increased. The sheet carrier concentration is also increased with implanted silicon ion dose. The highest electrical activation of 87 % occurred in $Al_{0.1}Ga_{0.9}N$ implanted with $1x10^{14}\, cm^{-2}$ silicon ions annealed at 1250 °C for 20 minutes. However, this caused damage due to nitrogen dissociation. The optimal conditions to maximize electrical activation and mobility for the $Al_{0.1}Ga_{0.9}N$ samples occurred when the samples were annealed at 1200 °C for 40 minutes. Electrical activation efficiencies of 82.6 and 83.5% were observed for silicon ion doses of $1x10^{13}$ and $5x10^{13}\, cm^{-2}$, respectively. At these anneal conditions the electrical activation of the sample implanted with $1x10^{14}\, cm^{-2}$ silicon ions was 75%.

48

However, the visual nitrogen dissociation damage is decreased and mobility stayed almost the same. The Electrical activation of the implanted ions in the sample doped with $1x10^{13}$ cm^{-2} silicon was poor for all anneal conditions but 1200 °C for 40 minutes.

A 500 Å protective layer of AlN was placed on $Al_{0.2}Ga_{0.8}N$ wafers which were implanted at room temperature with silicon ion doses ranging from $1x10^{13}$ to $1x10^{14}$ cm^{-2} at an energy of 200 keV. The samples were annealed at temperatures ranging from 1150 to 1350 °C for 20 minutes to determine optimum anneal temperature. Electrical activation efficiencies of 98.7 and 97.8% were obtained in $Al_{0.2}Ga_{0.8}N$ samples having ion doses of $5x10^{13}$ and $1x10^{14}$ cm^{-2} and annealed for 20 minutes at 1350 and 1300 °C, respectively. The highest mobility for $Al_{0.2}Ga_{0.8}N$ was 75.7 cm^2/V·s for the sample having an ion dose of $1x10^{14}$ cm^{-2} and annealed at 1350 °C for 20 minutes. Sheet carrier concentration in $Al_{0.2}Ga_{0.8}N$ increased with implanted ion dose. As anneal temperature increased the samples showed higher sheet carrier concentrations up to 1350 °C. For anneal temperatures at or below 1250 °C, mobility increased with anneal temperature. The results of this research compare well with past work with $Al_{0.2}Ga_{0.8}N$. An activation efficiency of 97.8% was obtained in $Al_{0.2}Ga_{0.8}N$ having an ion dose of $1x10^{14}$ cm^{-2} and annealed for 20 minutes at 1300 °C; this compares to previous work which found an activation efficiency of 60% when $Al_{0.2}Ga_{0.8}N$ was annealed at 1350 °C for 2 minutes [8:46]. The activation efficiencies observed in $Al_{0.2}Ga_{0.8}N$ samples having ion doses of $5x10^{13}$ and $1x10^{14}$ cm^{-2} and annealed for 20 minutes at 1350 and 1300 °C are greater than or equal to efficiencies reached using higher doses in $Al_{0.18}Ga_{0.82}N$ and GaN [3:6277;2:1930].

49

Observed Hall Mobilities in implanted $Al_{0.2}Ga_{0.8}N$ are greater than what has been obtained in past work. Hall Mobilities of 68.8 and 75.7 $cm^2/V{\cdot}s$ were obtained in $Al_{0.2}Ga_{0.8}N$ samples having ion doses of $5x10^{13}$ and $1x10^{14} cm^{-2}$ and annealed for 20 minutes at 1300 and 1350 ºC respectively. These Hall Mobilities are slightly greater than Hall Mobilities obtained in $Al_{0.18}Ga_{0.82}N$ samples at much higher doses of $1x10^{15} cm^{-2}$ 200keV silicon ions annealed at 1250 ºC for 25 minutes[3:6279]. Hall mobility of the $1x10^{14} cm^{-2}$ sample is 45 $cm^2/V{\cdot}s$ greater than previous results with the same ion dose annealed at 1350 ºC for 2 minutes[8:44].

Sample Cleaning Procedures

Cleanroom:

1. Return to cleanroom and turn solvent hood hotplate ON and set to 100 oC; Place all cutting disks face-up on hotplate
2. Set out as many 2" diameter pitri dishes with covers as you have source wafers and fill each ~. full w/ acetone.
3. Once crystal bond has been sufficiently softened, carefully remove each sample and place all pieces from each source wafer in their own pitri dish *** Organization is crucial to keeping track of which samples are which! ***
4. Once all the pieces are soaking in covered dishes of acetone, turn OFF the hotplate.
5. Add DI water to each dish with a ratio of acetone: DI of about 3:1 to aid in removing the ceramic disk residue.
6. Fill the ultrasonic cleaner with DI water to the level of fluid in each pitri dish.
7. Place each dish in the ultrasonic cleaner simultaneously ONLY if you can tell them apart, and ultra for 20 seconds.
8. Remove dishes from the cleaner; carefully flush each dish with clean acetone and cover.
9. Clean each piece one at a time—holding with tweezers, rinse with acetone, methanol, and DI water, blowing dry w/N2 and immediately placing in the appropriate glassine envelop prepared beforehand.
10. Once all the samples and remaining source wafers (and remnants) have been cleaned and packaged, clean all quartzware with acetone and methanol-- wiping will likely be necessary due to the PR, crystal bond and ceramic residue.

Oxy-Gon Sample Preparation Procedures

1. Select all the 5 mm x 5mm samples (which were previously cut & cleaned) you'll anneal.
2. On the cleanroom table, place a clean 3" Si wafer on a cloth wipe.
3. While holding them face down on the Si wafer, uniquely scribe the Al_2O_3 backside of each sample type (e.g., " / ", " < ", " | ", "O", "L", etc.)
4. Logically (e.g. hot and cold of same dose) and physically (e.g., best size match) pair up the samples.
5. After scribing, place all samples to be annealed in a 2" pitri dish for temporary storage and transport.

6. Measure out ~ 1¾" of Ta-wire for each sample pair to be annealed, cutting one long piece.
7. Place this single piece of Ta-wire in a 2" pitri dish, submerge the wire in TCE, and cover the dish.
8. Clean all samples again (front and back) with acetone and methanol rinses (and, as
9. necessary to fully remove ceramic disk residue and make each surface mirror-like, DI H2O), blow dry with N2. Rinse and flush the Ta-wire in the dish with acetone, then methanol. While still wet, pull the wire between a clean cloth wipe to dry.
10. Cut the wire into 1¾" sections.
11. Identify which samples will be wrapped face-to-face noting which sample will be on top.
12. Note: Practicing this process several times on a pair of junk samples is recommended.
13. Place a piece of Ta-wire on a cloth wipe and center the face-to-face samples in the middle of the wire.
14. Using two sets of tweezers, press the center of the samples together while wrapping the ends of the wire up and back across the top of the samples.
15. Bend first one end of the wire 90o at the center of the samples across the other wire, then bend the other end 90o so they interlock (like string on a Christmas package, or twine on a bail of hay).
16. Flip the sample pair over and repeat steps 14-15.
17. Flip the sample pair over and repeat steps 14-15 again, at which point you should have just enough wire to complete the final bends (step 15), only here interlock the ends and bend 180o vice 90o.
18. Keep the samples fully face-to-face throughout the process and wrap them securely. Any uncovered regions along the edge will be destroyed by the anneal—the samples must overlap perfectly!
19. Place the sample pair in the glassine envelope of the sample that started (and finished) on top.
20. Repeat steps 13-19 for each sample pair.
21. Place all the glassine envelopes in a plastic box and double bag for transport to anneal furnace.
22. Be sure to bring tweezers, gloves, wipes, and a metal dish for transport to/from the furnace.

Oxy-Gon AlN/GaN Anneal Procedures

System Start-Up:

1. Turn on Nitrogen gas and facility air.
2. Turn on "Main" power switch.
3. Make sure isolation valve is in the open.
4. Open load chamber door.

5. Place the specimen onto specimen holder (hearth). Check O-ring on door of load chamber.
6. Close and secure the load chamber door.
7. Turn on the roughing pump. Wait 2 minutes.
8. Press "Standby".
9. When vacuum TC-2 reaches 10^{-2} Torr, turn on the turbo pump. Allow the turbo pump to come up to operating speed (green light on turbo controller).
10. Press "Evacuate". With the Isolation valve open, this will allow both the load chamber and the furnace chamber to be evacuated.
11. When vacuum TC-1 is less than 9×10^{-2} Torr, the roughing valve will close. After a 2 second delay, the fore-line valve will openfollowed by the high vacuum valve.
12. When TC-1 reads less than 1×10^{-3} Torr, wait 5 minutes, and then turn on the ion gauge (press the "EMIS" button on the gauge controller).
13. When the chamber reaches a pressure less than 5×10^{-5} Torr, turn off the ion gauge and press the "Backfill" button. (V1 and V2 will open and the yellow indicators for each will illuminate.)
14. Open the flow meters in order to allow the chambers to achieve 2.0 PSIG (PS-1 and PS-2 yellow indicators for each chamber will illuminate).
15. Reduce the gas flow. Set flow meters for 2.0 LPM.
16. Press "Evacuate"
17. Repeat steps #13 thru #15.
18. Backfilling will continue through the annealing process.
19. Open water valve on the floor, wait 1 minute then turn "ON" heat zone.
20. Close isolation valve and bottom shields.
21. Put temperature control in "Auto". Set controller to desired temperature. The oven will heat according to the ramp rate. Currently set for 100°C/min.
22. When desired temperature is reached and stabilized open the isolation valve and the bottom shields.
23. Press the "Hearth Up" button to move the samples into the oven chambers. When the hearth is in place, close the bottom shields and turn the "Isolation Valve" switch into the "Closed" position.
24. At the end of the annealing process open the bottom shields and press the "Hearth Down" button. The samples will lower into the load chamber. The isolation valve will automatically close after the samples have been lowered into the load chamber.
25. Close the "Bottom Shields".
26. Make sure that the system is continuing to backfill during cooling. Allow your samples to cool to 25°C before opening the load chamber.
27. Load next samples. Check O-ring seal on the load chamber door. If it appears that it is dry some high vacuum grease should be applied.
28. Backfill the load chamber.
29. Open the flow meters in order to allow the chambers to achieve 2.0 PSIG (PS-1 and PS-2 yellow indicators for each chamber will illuminate).
30. Reduce the gas flow. Set flow meters for 2.0 LPM.

31. Press "Standby".
32. Press "Evacuate".
33. When the chamber reaches a pressure less than 5×10^{-5} Torr, turn off the ion gauge and press the "Backfill" button. (V1 and V2 will open and the yellow indicators for each will illuminate).
34. Open the flow meters in order to allow the chambers to achieve 2.0 PSIG (PS-1 and PS-2 yellow indicators for each chamber will illuminate).
35. Reduce the gas flow. Set flow meters for 2.0 LPM.
36. Open the isolation valve and bottom shields.
37. Press the "Hearth Up" button to move the samples into the oven chambers. When the hearth is in place, close the bottom shields and turn the "Isolation Valve" switch into the "Closed" position.
38. At the end of the annealing process open the bottom shields and press the "Hearth Down" button. The samples lower into the load chamber. The isolation valve will automatically close after the samples have been lowered into the load chamber.
39. Close the bottom shields.
40. Make sure that the system is continuing to backfill during cooling. Allow your samples to cool to 25ºC before opening the load chamber.

Shutdown- After samples have been removed:

1. Turn off the heat zone.
2. Open the isolation valve and the bottom shields.
3. Allow heat zone to cool down to room temperature.
4. At 100°C or lower the facility water can be shut off.
5. Press "Standby".
6. Press "Back fill"- allow chambers to achieve equal pressure.
7. Press "Standby" and let the oven temperature drop to below 30°C.
8. Close isolation valve and heat shields.
9. Turn off the turbo pump.
10. Turn off the mechanical pump.
11. Shutdown "Main" power
12. Turn off the nitrogen gas and facility air

Post-Anneal Contact Preparation Procedures

13. Obtain HCl and HNO3 acids and place within the acid fume hood
14. Turn ON one solvent fume hood hotplate and set to 140 oC
15. Turn ON the second solvent fume hood hotplate and set to 90 oC.
16. Fill a clean 250 ml quartz beaker with 50 ml of DI H2O; cover and place on the 140 oC hotplate.

54

17. On the cleanroom table, place an annealed Ta-wire-wrapped sample pair on a clean cloth wipe.
18. Using two sets of tweezers, carefully break off the brittle Ta wire-wrap, keeping track of which sample is which throughout the process.
19. Visually examine the AlN surface for signs of Ga droplets, cracking/peeling etc. (A good AlN surface post anneal will be as mirror-like as when it was wrapped.)
20. If the identifying scribe markings on the backside are no longer clearly distinguishable (at any angle or over a reflective Si wafer) place the sample on a clean 3" Si wafer and re-scribe.
21. Place the samples in a 2" pitri dish for temporary storage and transport.
22. Repeat steps 4-8 for each sample pair you have annealed.
23. Weigh out 1.63 g of KOH pellets (86% KOH) and tightly close the double bag.
24. Quickly place all pellets into the beaker of hot DI H2O as the pellets will begin to melt in air.
25. Stir with tweezers until all pellets are fully dissolved and cover the beaker. (Although the hotplate is set at 140 oC, the DI H2O will not boil, typically reaching at most 95 oC.)
26. *** Note: ensure the evaporator is not in use before proceeding with any acid processing.
27. Measure out 30 ml of HCl and place in a clean 250 ml quartz beaker.
28. Measure out 10 ml of HNO3 and add to the HCl; gently circulate and cover the aqua regia.
29. Process ONLY the good morphology samples as the first batch (< 5-10% total metallic Ga surface area is good). Process all other samples in the second batch.
30. Place each sample in the 0.5M hot KOH solution; starting a 5 min timer on the first sample. Use a 10minutes timer for $Al_xGa_{1-x}N$.
31. Continue placing samples one at a time at the same rate in the KOH sequentially along the circumference of the beaker and cover when finished.
32. When the samples have only 1 minute left in the KOH, bring the covered beaker of aqua regia to the solvent fume hood and place on the 90 oC hotplate.
33. At 5 minutes, remove the samples at the same rate and in the same order in which you inserted them.
34. As each sample is removed, place it into a large (600 ml) beaker of clean DI H2O.
35. Carefully rinse the samples in the beaker by dumping most of the DI/adding clean DI, dumping/adding—taking care to not even come close to loosing any samples. Leave at most 1" of DI in beaker.
36. When the aqua regia just begins to boil, place the samples into the acid solution directly from the DI beaker; starting a 2 minute timer on the first sample.
37. Continue placing samples one at a time at the same rate in the aqua regia sequentially along the circumference of the beaker and cover when finished.

38. At 2 minutes, remove the samples at the same rate and in the same order in which you inserted them.
39. As each sample is removed, place it into a large beaker of clean DI H2O.
40. When all the samples are in the DI, cover the aqua regia and turn off the 90 oC hotplate.
41. At this point, you may need to rinse a green residue off the metal tweezers, wipe, rinse and blow dry with N2
42. Carefully rinse the samples in the beaker by dumping most of the DI/adding clean DI, dumping/adding—taking care to not even come close to loosing any samples. Leave at most 1" of DI in beaker.
43. Holding with tweezers, agitate each sample in the DI, remove, blow dry with N2 and place in a clean 2" pitri dish.
44. Repeat steps 18-31 for the second batch as necessary using the same acid and base solutions.
45. On the cleanroom table, carefully mount all samples face down on the van der Pauw shadow mask on a clean cloth wipe.
46. Adjust and secure each sample by gently tightening mounting screws until all samples are positioned for contacts as much in the corners as possible.
47. Note: Each row on the mask is a different sized square; generally the largest two square rows are best.
48. *** Note: This is an iterative and tedious process as tightening one sample may loosen another. ***
49. When all samples are securely squared, vent the evaporator and carefully insert the mask.
50. Remember to change the microscope window slides, check metal levels, secure door and "process".
51. Turn off both hotplates, clean up all acids, bases, DI, Ta-wire-pieces, etc.

Edwards Auto 306 Evaporator Procedures

Sample preparation:

1. Degrease sample with solvents (acetone, methanol) DI rinse and N2 blow dry
2. Remove any oxides with 2 minutes of boiling aqua regia (HNO3:HCl, 1:3), DI rinse and N2 blow dry

Vent chamber, Mount/Remove sample & Create vacuum:

1. Ensure chamber is not in use and has been cooled for at least ½ an hour after the last evaporation.
2. Press "Seal/Vent" and lift chamber clip—door will open easily at 7.6E2 Torr—not until.
3. When vented, open chamber door and remove sample jig—if removing, do so & go to Step 7.

4. Mount cleaned sample(s) properly on jig
5. Physically verify the metals in each carousel positions and note for assigning layer parameters.
6. Check amount of metal in hearths to be used and fill only as necessary—half full is OK.
7. Insert jig into chamber, and secure door.
8. Press "Process" to start vacuum.
9. Fill liquid N2 reservoir to improve pump-down time.
10. Confirm metal parameters on each layer to be used (density, tooling, z-factor, etc.).
11. Program the thickness for each layer in nm.

Evaporation:

1. Wait until vacuum = 2×10^{-7} Torr is obtained
2. Turn electron Gun Power Supply ON.
3. Turn gun and on/off ON, and wait for lights (Power, Vac, H2O, Rot, Gun, Local, and Beam).
4. Check ~4.85 kV high voltage setting and 15-17 oC water chiller.
5. Using Data button, select appropriate layer and confirm settings changing as necessary.

	Ti	Al	Au	Ni
Layer	1	4	2	3
Density	4.5	2.7	19.3	8.91
Z-factor	14.1	8.2	23.2	26.6
Tooling	0.85	0.85	0.85	0.85
Beam for evap	120 mA	45 mA	120 mA	125mA

6. Ensure shutter is closed and no shutter control buttons are pushed.
7. Activate Beam Sweeping by setting control knob to "1".
8. Turn Beam Current control knob to 1st notch (~ 20 mA).
9. Slowly ramp Beam Current up in 20 mA steps every several seconds, monitoring vacuum pressure—don't let pressure exceed 1×10^{-5} Torr.
10. If metal has not been used recently, evaporate off impurities by getting metal liquid hot (i.e., at the onset of evaporation—watch for solid to liquid phase change) otherwise go to step 12.
11. As necessary, allow chamber to return to 2×10^{-7} Torr, then repeat starting at step 9.
12. Stop ramping Beam Current when desired beam current is achieved, or turn down if 9×10^{-6} Torr is exceeded.
13. Arm shutter by depressing Remote button
14. Press "Run" to open shutter and start evaporation, noting start time.
15. Watch deposition rate and pressure; modify Beam Current to keep both within proper limits.
16. Log time when deposition completes.

17. Turn Beam Current down slowly (2-3 seconds) to zero.
18. Activate Carousel and move to position of next metal, else go to step 21 if done evaporating.
19. Using Data button, select appropriate layer and confirm settings changing as necessary.
20. Go to Evaporation step 8 when chamber returns to 2x10-7 Torr
21. Deactivate Beam Sweeping, Carousel, and disarm shutter Remote.
22. Turn gun and on/off OFF, turn Gun Power Supply OFF.
23. Log evaporation results into the Evaporation log book.
24. Wait at least ½ hour and follow vent procedures.

Probe Station Operating Procedures

System Start-Up

1. Turn on vacuum and nitrogen gas under probe station.
2. Turn on computer and monitor.
3. Turn on video camera.
4. Turn on microscope light above probe station.
5. Turn on HP 41501A and 4155A units.

Probe and Connection Configuration

1. Use the triax connector probes only.

2. Must be connected to ports 1 and 3.

Electrical Setup

1. Press MEM4 on 4155A for diode measurements.
2. Use SMU1 and SMU3.
3. Under the "Page Control" section press the "Chan" button (press "Chan" button anytime to return to this setup page).
4. Press "Meas".
5. Choose single sweep.
6. Press arrow up and down keys to move to start.
7. Enter start voltage±.
8. Enter stop voltage±.
9. Step size is variable from 100 µV to 100 milli volt is typical.
10. Compliance is the maximum current limit applied to the device.
11. Press (under "Page Control") "Display".
12. Use arrow down to move through options.

58

13. Enter min start and max stop voltages.
14. Press display when finished.

Sample Setup

1. Put sample on vacuum stage over small centered opening.
2. Flip toggle switch to apply vacuum (located on the left side of the instrument).
3. Place probes on sample.
4. Press "single on the measurements panel.
5. Use default computer display program.

Shut down

1. Remove test sample.
2. Turn off all equipment including camera and lamp
3. Shut off nitrogen gas and vacuum

59

Bibliography

[1]   Cao, X. A. et al. Applied Physics Letters. Vol 73,1998.

[2]   Fellows, James A., Yung K. Yeo, Robert. L. Hengehold, and D. K. Johnstone, Applied Physics Letters. Vol 80, (2002).

[3]   Ryu, Mee-Yi, Yung K. Yeo, and Robert. L. Hengehold, Journal of Applied Physics. Vol 96, Num 11 (2004).

[4]   Ahoujja, M., et al. "Electrical and Optical Investigation of MBE grown Si- Doped AkGaN as a Function of Al Mole Fraction up to 0.5," Materials Science and Engineering B91-92: 285 (2002)

[5]   Morkoc, H., et al. "Large-band-gap SiC, III-V Nitride, and II-IV ZnSe-based semiconductor Device Technology", J. App. Phys., 76:1363 (1994)

[6]   Bhattacharya, Semiconductor Optoelectronic Devices 2nd ed, New Jersey: Prentice Hall, 1997.

[7]   Claunch, Erin N. "Luminescence Studies of Ion-Implanted Gallium Nitride and Aluminum Gallium Nitride", Wright-Patterson AFB, OH: Air Force Institute of Technology (2001).

[8]   Chitwood, Elizabth A. "Electrical Activation Studies of Silicon Implanted AlxGa1-xN and Coimplanted GaN", Wright-Patterson AFB, OH: Air Force Institute of Technology (2003).

[9]   Ryu, Mee-Yi. "Excellent Electrical Activation Efficiency Obtained from Si-implanted Al0.18Ga0.82N": Interim Report. Dayton OH: University of Dayton Research Institute

[10]   Borges, Ricardo. "GaN High Electron Mobility Transistors." Nitronex Status of Research Report. n. pag. http://www.nitronex.com/education/ganHEMT.pdf. 07 Jan 2005.

[11]   Zou, J, D. Kotchetkov, F. Pollak, Thermal conductivity of GaN films: Effects of Impurities and Dislocations, Journal of Applied Physics. Vol93(5) , (2002), 2534-2539.

[12]   McKelvey, Solid State Physics, Florida: Krieger Publishing Company, 1993

[13]   Sze, S. M. Physics of Semiconductor Devices (2nd edtion). New York: John
        Wiley and Sons, 1981

[14]   Pankove, Optical Processes in Semiconductors, New Jersey: Dover
        Publications,1971

[15]   Suzuki, M, T. Uenoyama, A. Yanase, First-principles calculations of effective-
        mass parameters of AlN and GaN, Phys. Rev. B 52, 11 (1995), 8132-8139.

[16]   Gorczyca, I., Christensen N.E., Phys. B 185 (1993), 410-414. Gorczyca, I., Svane
        A., Christensen N.E., Internet J. Nitride Sem. Res. 2, Article 18 (1997).

[17]   Fellows, James A. "Electrical Activation Studies Ion implated Gallium Nitride",
        Wright-Patterson AFB, OH: Air Force Institute of Technology (2001).

REPORT DOCUMENTATION PAGE		Form Approved OMB No. 074-0188

The public reporting burden for this collection of information is estimated to average 1 hour per response, including the time for reviewing instructions, searching existing data sources, gathering and maintaining the data needed, and completing and reviewing the collection of information. Send comments regarding this burden estimate or any other aspect of the collection of information, including suggestions for reducing this burden to Department of Defense, Washington Headquarters Services, Directorate for Information Operations and Reports (0704-0188), 1215 Jefferson Davis Highway, Suite 1204, Arlington, VA 22202-4302. Respondents should be aware that notwithstanding any other provision of law, no person shall be subject to an penalty for failing to comply with a collection of information if it does not display a currently valid OMB control number.
PLEASE DO NOT RETURN YOUR FORM TO THE ABOVE ADDRESS.

1. REPORT DATE (DD-MM-YYYY) March 2005	2. REPORT TYPE Master's Thesis	3. DATES COVERED (From – To) April 2004 – Feb 2005

4. TITLE AND SUBTITLE	5a. CONTRACT NUMBER
Electrical Activation Studies of Silicon Implanted $Al_xGa_{1-x}N$	5b. GRANT NUMBER
	5c. PROGRAM ELEMENT NUMBER
6. AUTHOR(S)	5d. PROJECT NUMBER
Zens, Timothy, W., 2nd Lieutenant, USAF	5e. TASK NUMBER
	5f. WORK UNIT NUMBER

7. PERFORMING ORGANIZATION NAMES(S) AND ADDRESS(S) Air Force Institute of Technology Graduate School of Engineering and Management (AFIT/EN) 2950 Hobson Way WPAFB OH 45433-7765	8. PERFORMING ORGANIZATION REPORT NUMBER AFIT/GAP/ENP/05-08
9. SPONSORING/MONITORING AGENCY NAME(S) AND ADDRESS(ES) N/A	10. SPONSOR/MONITOR'S ACRONYM(S)
	11. SPONSOR/MONITOR'S REPORT NUMBER(S)

12. DISTRIBUTION/AVAILABILITY STATEMENT
APPROVED FOR PUBLIC RELEASE; DISTRIBUTION UNLIMITED

13. SUPPLEMENTARY NOTES

14. ABSTRACT

Electrical activation studies of silicon implanted $Al_xGa_{1-x}N$ grown on sapphire substrates were conducted as a function of ion dose, anneal temperature, and anneal time. Silicon ion doses of $1x10^{13}$, $5x10^{13}$, and $1x10^{14}$ cm^{-2} were implanted in $Al_xGa_{1-x}N$ samples with aluminum mole fractions of 0.1 and 0.2 at an energy of 200 keV at room temperature. The samples were annealed at temperatures 1100 to 1350 °C and anneal times 20 to 40 minutes. The Hall coefficient and resistivity were measured using room temperature Hall effect measurements.

Activation efficiencies of almost 100% were achieved for $Al_{0.2}Ga_{0.8}N$ samples having doses of $5x10^{13}$ and $1x10^{14}$ cm-2 after annealing at 1350 and 1300 °C, respectively, for 20 minutes. After annealing at 1250 °C for 20 minutes, 87% efficiency was achieved for $Al_{0.1}Ga_{0.9}N$ implanted with $1x10^{14}$ cm^{-2} silicon ions. The largest mobility was 89 cm2/V·s for $Al_{0.1}Ga_{0.9}N$ implanted with $1x10^{14}$ cm^{-2} and $5x10^{13}$ cm-2 silicon ions and annealed at 1250 °C for 20 minutes and at 1200 °C for 40 minutes, respectively.

The optimal anneal condition to maximize electrical activation efficiency and minimize nitrogen dissociation damage for $Al_{0.1}Ga_{0.9}N$ was 1200 °C anneal for 40 minutes. The mobilities, sheet carrier concentrations, and electrical activation efficiencies generally increased

15. SUBJECT TERMS
Activation, Ion Implantation, Aluminum Nitrides, Gallium Nitrides, Annealing, Mobility, Concentration, Silicon..

16. SECURITY CLASSIFICATION OF:			17. LIMITATION OF ABSTRACT	18. NUMBER OF PAGES	19a. NAME OF RESPONSIBLE PERSON Dr. Yung Kee Yeo, Civ AFIT/ENP
a. REPORT U	b. ABSTRACT U	c. THIS PAGE U	UU	73	19b. TELEPHONE NUMBER (Include area code) (937) 785-3636, ext 4532; e-mail: yyeo@afit.edu

Standard Form 298 (Rev: 8-98)
Prescribed by ANSI Std. Z39-18